Clustered Seismicity in Alabama: Natural or Anthropogenic?

by

Jian Chen

A thesis submitted to the Graduate Faculty of
Auburn University
in partial fulfillment of the
requirements for the Degree of
Master of Science

Auburn, Alabama
August 5, 2017

Keywords: Clustered seismicity, Natural earthquake, Induced earthquake, Earthquake location, Earthquake detection, Focal mechanism

Approved by

Lorraine W. Wolf, Chair, Professor of Geosciences
Nedret Billor, Professor of Statistics
Ming-Kuo Lee, Professor of Geosciences
Mark G. Steltenpohl, Professor of Geosciences

Abstract

Seismicity in the central and eastern U.S. is typically characterized by low-magnitude earthquakes (M < 4) with a random distribution that occur in areas of low to moderate strain rates. An unprecedented increase in earthquakes in the central and eastern U. S. since 2009 has been attributed to operations related to resource extraction. Since November 2014, an earthquake swarm consisting of 21 earthquakes in northwestern Greene County, Alabama, has been recorded. The magnitudes of these earthquakes are small, less than 3.8, with many earthquakes only lightly felt by residents in the area. The source of the seismicity is unknown. This study intends to investigate the spatiotemporal and waveform characteristics of the Greene Country earthquake cluster to explore its possible source and the physical mechanism responsible for their occurrence.

After spatiotemporal and waveform characteristics analysis, anthropogenic activities including underground injection, oil and gas extraction, mining extraction, quarrying operations, and sinkhole formation are likely not the cause of the swarm, even though they cannot be unequivocally ruled out. While recent research has demonstrated an unequivocal link between resource recovery processes and seismicity, regional tectonic processes and geologic structures are also responsible for seismicity. Consequently, this study favors the interpretation that the earthquakes may represent a continuation or southwesterly migration of the Southern Appalachian seismic zone (SASZ), because the Greene County cluster follows a northeasterly

trend and earthquake focal mechanisms consistently indicate right-hand lateral motion on NNE-trending planes, which is consistent with previous investigation.

Acknowledgments

I would like to take this chance to express my greatest appreciation to my adviser, Dr. Lorraine Wolf, whose kind and constant support of this project made its completion possible. Without her motivation, encouragement, consistent guidance and expertise, I would still be wandering. My deepest gratitude also goes to my other committee members Dr. Mark Steltenpohl, Dr. Ming-Kuo Lee, and Dr. Nedret Billor. Thank you all for your patience, expertise, support, and insightful comments to this research.

Moreover, my gratitude also extends to the rest of the faculty members, staff, and graduate students in the Department of Geosciences at Auburn University, who provided the necessary support and assistance. I would like thank other people who helped me at various times throughout my research. Great thanks to Dr. Charlotte Rowe and Dr. Heather DeShon for commenting on my research. I would like to especially thank everyone at the Geological Survey of Alabama and State Oil and Gas Board: Dr. William Thomas, Dr. Sandy Ebersole, Mr. Butch Gregory, Mr. William Jackson, and Ms. Camilla Musgrove. Your willingness to speak with me and provide me with resources was crucial to this research.

Last but not least, I would like to send out all of the love and appreciation that I could for my parents, my brother, as well as my wife, Rongting Xu. The support they have shown me throughout my life will never be eclipsed, and my gratitude is endless.

Table of Contents

Abstract ii

Acknowledgments iv

Table of Contents v

List of Tables vi

List of Figures vii

Introduction 1

Geologic setting 6

Historical seismicity 9

Data and processing 13

- Data collection 13
- Earthquake relocation 16
- Earthquake detection 19
- Focal mechanism analysis 25

Discussion of possible sources 29

Conclusions 37

References 38

List of Tables

Table 1. Historical seismicity in Greene County area. 12

Table 2. Earthquakes for the northwestern Greene County from November 2014 to September 2016..... 14

Table 3. Velocity model used for earthquake relocation. 16

Table 4. Station key input used for subspace detection. 20

Table 5. Template key input used for subspace detection (for temporarily deployed station EUAL, only 4 events were recorded during three months). 21

List of Figures

Figure 1. Earthquakes in the U.S. mid-continent from 1973 to 2014. (a) White and red dots denote earthquakes that are spatiotemporally non-associated and associated with injection wells, respectively. (b) Gray bars represent the number of $M \geq 3.0$ earthquakes per year in the U.S. midcontinent; red bars represent the number of earthquakes that are spatiotemporally associated with injection wells. Black line denotes the number of non-associated earthquakes per year. (from Weingarten et al., 2015)..... 2

Figure 2. Earthquake induced mechanism by injection. (a) When pore-fluid pressure $P = 0$, the effective stress $\sigma' = \sigma$. (b) When $P \neq 0$, $\sigma' = \sigma - \alpha P\delta_{ij}$, where α is the Biot-Willis coefficient and δ_{ij} is the Kronecker delta. (c) Mohr circle with Mohr–Coulomb failure envelope. (d) Earthquakes can be induced by changing the shear or normal stresses acting on the fault. (e) Earthquakes can also be induced by increasing the pore pressure acting on the fault. (from Sun et al., 2017) 3

Figure 3. Location of Greene County (gray) in BWB (blue). Also shown are tectonic elements and physiographic provinces. (revised from Hatch and Pawlewicz, 2007). 6

Figure 4. (A) Geologic map of Greene County (thick gray polygon). Basement faults include Paleozoic thrust faults (blue dashed lines) and Precambrian normal faults (red lines). Precambrian graben indicated by red hachured lines. Basement faults follow two trends, NE-SW and NW-SE. (B) General stratigraphy and structure interpreted from seismic reflection data and well logs along a cross-section extending through central part of Greene County (modified from Surles, 2007). 8

Figure 5. Seismic Zones of the Southeastern U.S. The Southern Appalachian Seismic Zone is located in the southwestern section of the NE-trending Appalachian Mountain belt, which extends from Virginia to Alabama. (from https://gsa.state.al.us/)..... 10

Figure 6. Historical seismicity around Greene County, Alabama. Epicenters of earthquakes in the Greene County cluster are represented by different sized stars. Labeled stars show the locations for earthquake epicenters before the cluster, with the date and magnitude in the label. Insert map shows the regional seismicity in north and central Alabama. Earthquake epicenters are represented by different sized stars. (from https://www.eia.gov/)..... 11

Figure 7. Regional seismic stations located within 400-km around the Greene County swarm. Green triangles represent stations in Central and Eastern US Network (N4), empty triangles represent stations in Cooperative New Madrid Seismic Network (NM), blue squares represent stations in United States National Seismic Network (US), and empty squares represent stations in

CERI Southern Appalachian Seismic Network (ET). Yellow dashed circles give the distance from the Greene County epicentral area. (from http://www.fdsn.org/networks/) 15

Figure 8. Earthquake relocation result for Greene County cluster. Black stars show the initial locations from USGS, blue squares show the relocated locations given by hypoinverse2000, and red dots show the final locations from HypoDD. Colored areas mark the average location uncertainties for HypoDD, Hypoinverse, and the original USGS locations. Cross sections show the depth variation of hypocenters projected into a vertical plane derived from HypoDD and dashed lines give the average depth. 18

Figure 9. Similarity matricies on each station (N4.Z47B and NM.EUAL); axes represent template ID (Temid) and colored squares represent similarity related to correlation coefficient for individual pairs..... 22

Figure 10. Dendrogram created to visualize grouping structure on each station, horizontal axis represents template ID (Temid) and vertical axis represents dissimilarity related to correlation coefficient. 22

Figure 11. Vertical components waveforms of template earthquakes on station EUAL and Z47B. 23

Figure 12. Vertical component waveforms of detected earthquakes on station EUAL and Z47B. Similarity among traces indicates a source is repeatedly ruptured. 25

Figure 13. Comparison between synthetic (red) and observed (black) seismograms for moment tensor inversion. The numbers on the lower left side of the seismograms are the time shifts (upper) and cross-correlation coefficient in percent (lower). Positive time shifts mean delay or right-shift of the synthetic seismograms. 28

Figure 14. Mines (http://www.surface-mining.state.al.us/), quarries and sand pits (http://quarriesandbeyond.org), and sinkholes (https://gsa.state.al.us/) in west-central Alabama. Yellow dashed circle indicates the 50 km distance from the Greene County epicentral cluster. . 30

Figure 15. Oil and Gas wells in north and central Alabama. Dashed circles indicate the 15 & 50 km distance from the Greene County cluster epicenter. Inserted map shows the enlarged area within the red rectangle. (Well status: AC – Active, PR – Producing. Well type: CM - Coal Bed Methane, GAS - Natural Gas, OIL – Oil, SHG - Shale Gas, SWD - Salt Water Disposal, UN – Undesignated). See text for discussion. (https://gsa.state.al.us/) 32

Figure 16. Preliminary focal mechanisms for the M > 3 events in Greene County swarm are shown. The focal mechanisms suggest right-lateral strike-slip motion on NE-oriented faults, or left-lateral strike-slip on NW-oriented faults. Labels of focal mechanisms indicate date of

earthquake. Basement faults are shown with lines; red lines indicate Precambrian normal faults and blue dashed lines represent Paleozoic thrust faults. (https://gsa.state.al.us/) 34

Introduction

Seismicity in the central and eastern U.S. is typically characterized by low-magnitude earthquakes ($M < 4$) with a random distribution (Frankel, 1995; Petersen et al., 2008) that occur in areas of low to moderate strain rates. Some exceptions are the large ($M > 7$) 1811-1812 earthquakes that occurred in the central U.S. (e.g., Tuttle et al., 2002) and the $M \sim 6.9$ 1886 Charleston earthquake (Bakun and Hopper, 2004). Periodic small earthquake swarms or clusters form part of the background activity, often having no association with active faults or geologic structures. In Alabama, some of these swarms have been associated with quarry activity, mine collapse and resource extraction.

The possibility that earthquakes can be induced by injection of fluids into the subsurface was established in the mid-1960s in a study aimed at determining the cause of seismicity close to the Rocky Mountain Arsenal near Denver, Colorado (Healy et al., 1968; Herrmann, et al., 1981). Despite the unequivocal connection between fluid injection and the Rocky Mountain Arsenal earthquakes, relatively few cases of earthquakes induced by wastewater injection were documented prior to 2009 because the hazard from these earthquakes was considered low (Petersen et al., 2008).

An unprecedented increase in earthquakes in the United States mid-continent since 2009 has been attributed to operations related to resource extraction (Ellsworth, 2013; Keranen et al., 2013). Within the central and eastern U.S., the number of earthquakes with magnitudes greater than or equal to 3 ($M \geq 3$) has increased dramatically over the past few years. Between the years

1970–2008, there was an average of 24 M ≥ 3 earthquakes in the central and eastern U.S. This rate jumped to an average of 193 M ≥ 3 earthquakes per year from 2009 to 2013, and the rate continues to rise. In 2014, there were more than 650 M ≥ 3 earthquakes, most of which were believed to be associated with injection (Figure 1; Rubinstein and Mahani, 2015; Weingarten et al., 2015). Magnitudes of this size are large enough to be felt by people, yet rarely cause damage. However, several damaging earthquakes thought to be related to resource recovery have occurred: the 2011 M 5.6 Prague, Oklahoma, earthquake; the 2011 M 5.3 Trinidad, Colorado, earthquake; the 2012 M 4.8 Timpson, Texas, earthquake; and the 2011 M 4.7 Guy, Arkansas, earthquake (Keranen et al., 2014; Barnhart et al., 2014; Frohlich et al., 2014; Horton, 2012). The increase in earthquake rate and the occurrence of damaging earthquakes have prompted the scientific community to focus efforts on understanding the hazard posed by injection-related earthquakes.

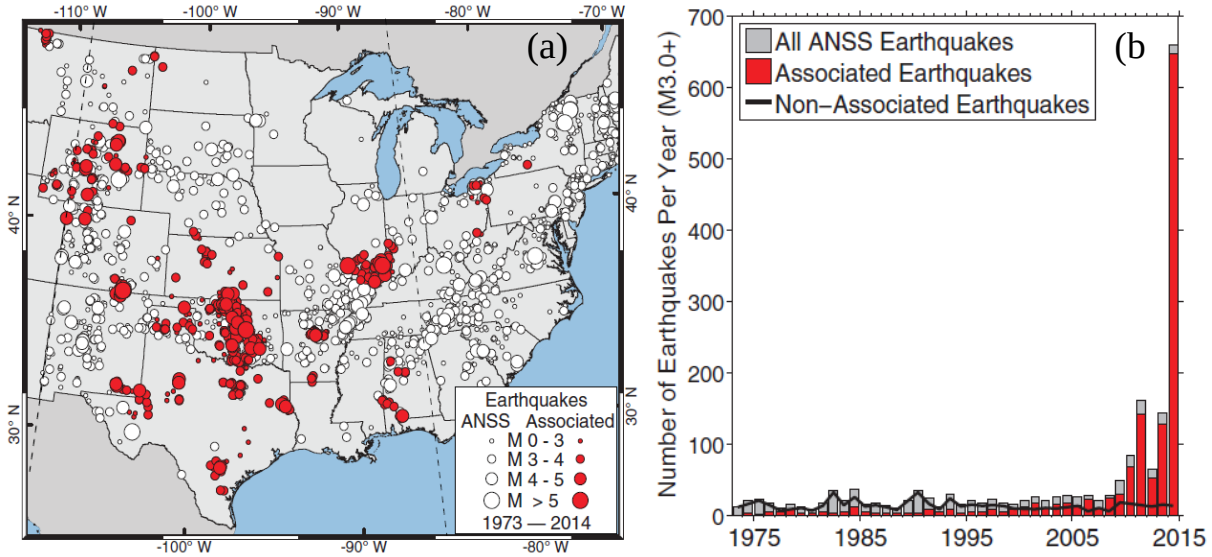

Figure 1. Earthquakes in the U.S. mid-continent from 1973 to 2014. (a) White and red dots denote earthquakes that are spatiotemporally non-associated and associated with injection wells, respectively. (b) Gray bars represent the number of M ≥ 3.0 earthquakes per year in the U.S. midcontinent; red bars represent the number of earthquakes that are spatiotemporally associated with injection wells. Black line denotes the number of non-associated earthquakes per year. (from Weingarten et al., 2015)

A number of scientists have attempted to determine if seismic activity is linked to injection in wells. Nicholson and Wesson (1990) described that, under certain circumstances, the increased pore pressure resulting from fluid injection, whether for waste disposal, secondary recovery, geothermal energy, or solution mining, can trigger earthquakes. Davis and Frohlich (1993) proposed criteria related to background seismicity, temporal and spatial correlation, and injection practices to form a descriptive profile of an injection project. The profiles of injection sites provide a convenient tool for determining whether an injection site closely resembles other sites where injection induces earthquakes. Ellsworth (2013), in his review of seismic activity that could be associated with industrial activity, focused on the disposal of wastewater by injection in deep wells. Earthquakes may be induced by increasing the pore pressure acting on a fault or by changing the shear and normal stress acting on a fault (Figure 2).

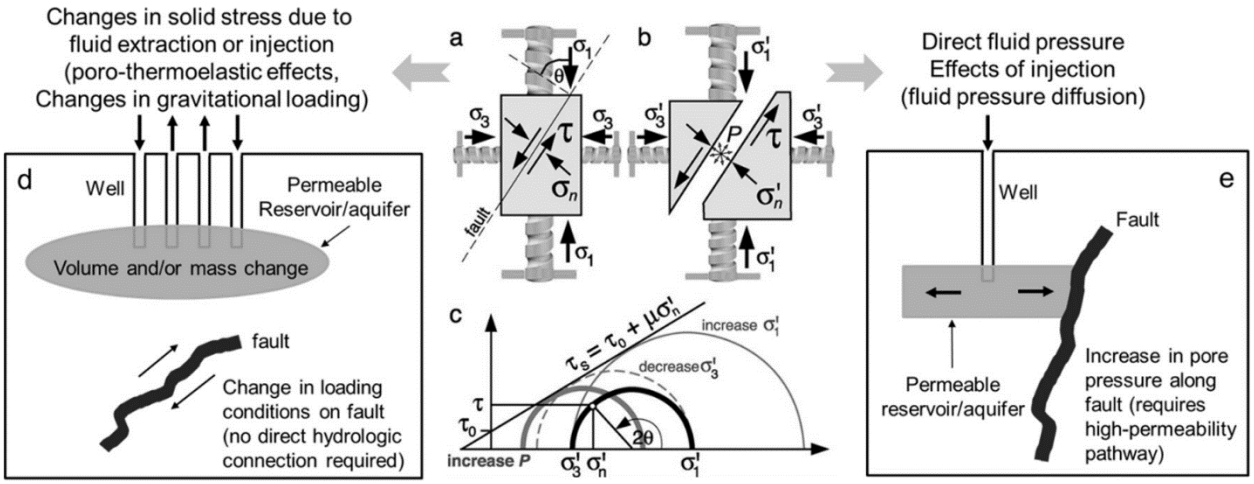

Figure 2. Earthquake induced mechanism by injection. (a) When pore-fluid pressure P = 0, the effective stress $\sigma' = \sigma$. (b) When $P \neq 0$, $\sigma' = \sigma - \alpha P \delta_{ij}$, where α is the Biot-Willis coefficient and δ_{ij} is the Kronecker delta. (c) Mohr circle with Mohr–Coulomb failure envelope. (d) Earthquakes can be induced by changing the shear or normal stresses acting on the fault. (e) Earthquakes can also be induced by increasing the pore pressure acting on the fault. (from Sun et al., 2017)

In the past few years, an unprecedented increase in seismicity rate in the central and eastern U.S. spawned a cascade of studies that sought to explore the mechanisms of induced seismicity. Keranen et al. (2014) used seismicity and hydrogeological models to show that fluid migration from high-rate disposal wells in Oklahoma is likely responsible for the largest swarms. Rubinstein and Mahani (2015) described wastewater injection as the primary cause of a large change in seismicity rate observed in the United States. Walsh and Zoback (2015) showed that increases in seismicity in Oklahoma (Cherokee, Perry, and Jones study areas) follow 5- to 10-fold increases in the rates of saltwater disposal. They discussed a conceptual model for Oklahoma seismicity that indicates significant increases in saltwater disposal will increase the pore pressure and eventually trigger slip on critically stressed basement faults. Göbel (2015) made a detailed comparison of injection parameters in Oklahoma and California, including well density, wellhead pressures, peak and cumulative rates, and injection depths, and found that the primary controls on injection-induced earthquakes appear to be the specific geologic setting, e.g., hydraulic connectivity, and the stress state on nearby faults. Dieterich et al. (2015) developed a method to simulate injection-induced seismicity that couples the regional scale, multicycle earthquake simulator to reservoir models that estimates changes in effective stresses on modeled faults due to fluid injection. The results of their study indicate that the space-time patterns of simulated injection-induced seismicity are quite sensitive to pre-injection fault stresses. Weingarten et al. (2015) examined the relationship between wastewater injection and U.S. mid-continent seismicity using a newly assembled injection well database for the central and eastern U.S. and found that the entire increase in earthquake rate is associated with fluid injection wells.

They conclude that wastewater disposal wells and high-rate injection wells (> 300,000 barrels per month) are much more likely to be associated with earthquakes than other wells.

Although few earthquakes are documented for Greene County, Alabama, before November 2014, a series of 21 notable yet unusual earthquakes has since occurred. The magnitude of these earthquakes is small, less than M 3.8, with many earthquakes only lightly felt by residents in the area. The source of the seismicity is unknown. The primary objective of this study is to investigate the spatiotemporal and waveform characteristics of the Greene Country earthquake cluster to explore its possible source and the physical mechanism responsible for their occurrence.

Geologic setting

Greene County is situated in the southern part of the Black Warrior Basin (BWB), a triangular-shaped foreland basin that straddles Alabama and Mississippi. BWB is bounded on the east and southeast by the Appalachian orogenic belt (Figure 3; Hatch and Pawlewicz, 2007). Paleozoic rocks in the basin range from Cambrian to Pennsylvanian age, mostly covered by Mesozoic clastic and carbonate sediments. Cenozoic units include Pleistocene terrace gravels and Quaternary alluvium (Raymond et al., 1988).

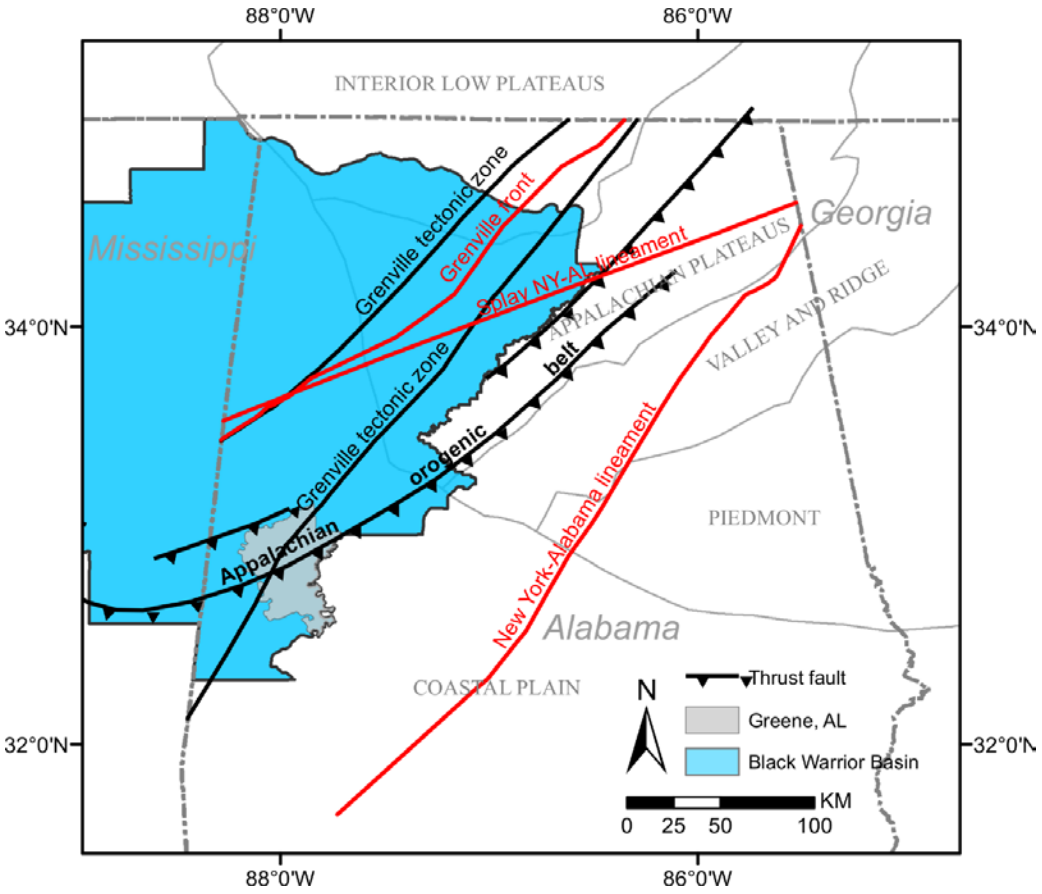

Figure 3. Location of Greene County (gray) in BWB (blue). Also shown are tectonic elements and physiographic provinces. (revised from Hatch and Pawlewicz, 2007).

Stratigraphic units underlying Greene County are covered by the sediments of the Gulf Coastal Plain, consisting of the Eutaw formation (Cretaceous sands, clays, and muds) and alluvial, coastal, and low-terrace deposits (Holocene alluvium and beach sand) (Figure 4A). Paleozoic rocks of the BWB are underlain by Precambrian Laurentian basement rocks. Structural elements in the basement rocks around Greene County, Alabama, include the Grenville front, the New York-Alabama lineament, two sets of basement faults system (one oriented NW-SE and another oriented NE-SW). Early Mesozoic rifting associated with the formation of the Gulf of Mexico and opening of the Atlantic Ocean resulted in numerous northwest- and northeast-trending normal faults and northeast-trending horsts and grabens (Figure 4; Raymond et al., 1988; Raymond et al., 2009).

Surles (2007) constructed a series of geologic cross-sections based on well logs and seismic reflection lines throughout the BWB. One of these crosses the central part of Greene County (Figure 4B). This cross-section characterizes the Blue Creek fault in the study area as a low-angle thrust fault that duplicates sedimentary strata within the basin sequence and merges with a master decollement at about 6 km depth. Below the decollement are normal-faults in the basement rocks that formed during extension associated with the break-up of Pangaea (Thomas, 2006). Wells along the cross-section terminate at the top of the Knox formation (~ 6400 m), below which the deep structure is based on the seismic reflection data.

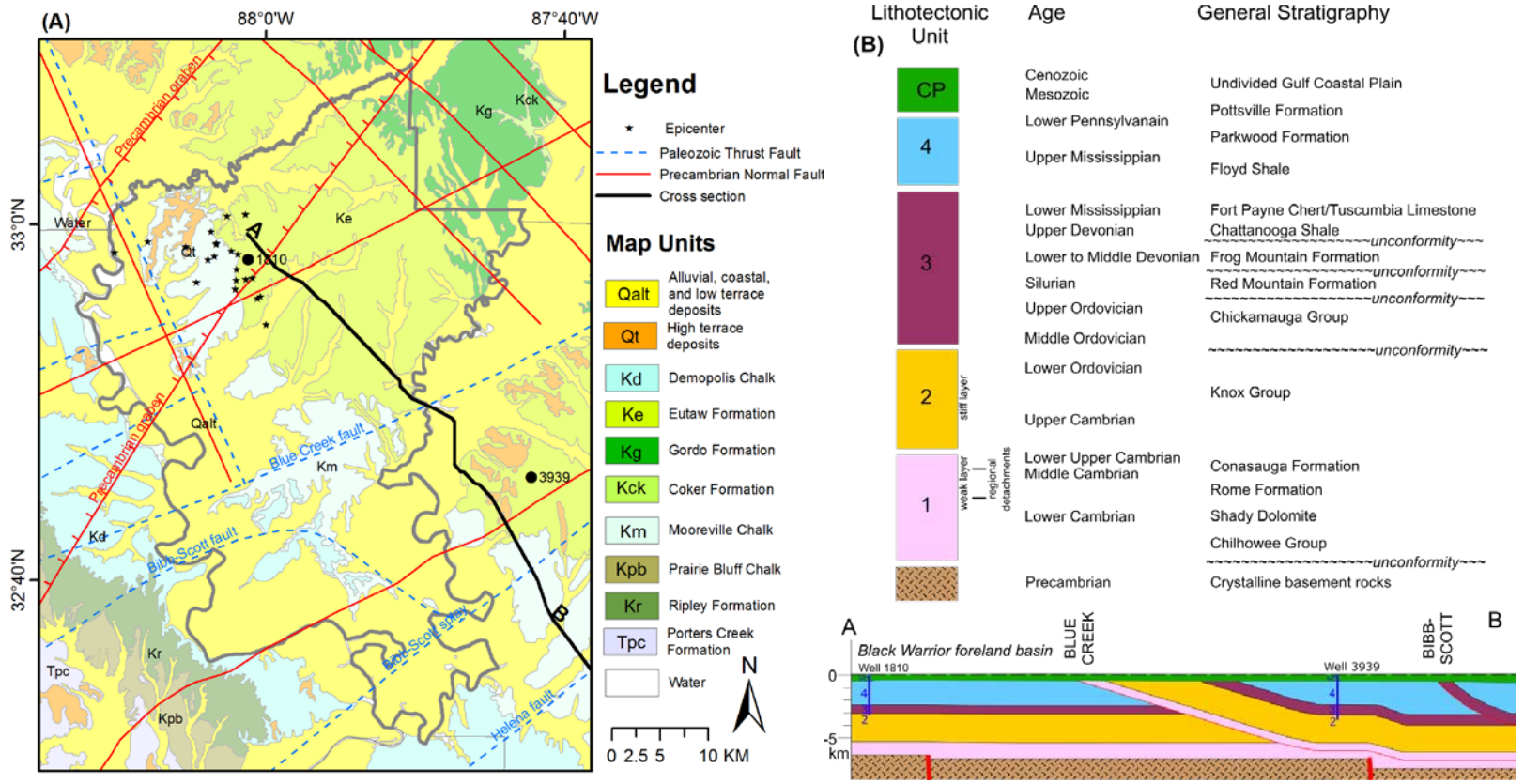

Figure 4. (A) Geologic map of Greene County (thick gray polygon). Basement faults include Paleozoic thrust faults (blue dashed lines) and Precambrian normal faults (red lines). Precambrian graben indicated by red hachured lines. Basement faults follow two trends, NE-SW and NW-SE. (B) General stratigraphy and structure interpreted from seismic reflection data and well logs along a cross-section extending through central part of Greene County (modified from Surles, 2007).

Historical seismicity

Historical seismicity data are needed to establish the background rate of naturally occurring events in a particular area over many decades or centuries, which, in turn, may indicate whether recent increases in seismicity are anomalous and perhaps induced by human activity. The historical seismicity record in the eastern U.S. is incomplete for small magnitude events (M < 3.0) because sufficient network coverage has only existed for the last decade. Lack of seismic stations often equates to no detected seismicity. Seismic station coverage across the United States since the 1970s is believed to be adequate for detecting all earthquakes of M 3.0 and above, although locations and depths may be highly uncertain. Although Alabama has hosted several temporary networks in the past, only one permanent station existed in the northwest corner of the state until 1980, when additional stations were added. Twenty-three seismic stations were temporarily located in Alabama beginning in 2011 as part of EarthScope's USArray (http://www.usarray.org/) campaign for two years. Although most were removed by 2014, several were retained to form a permanent network of nine stations.

The northern and north-central Alabama region is not considered to be in a high-risk area for significant damage caused by earthquakes (Petersen et al., 2015). However, because of proximity to the New Madrid seismic zone (NMSZ), there is a need to be aware of the potential for local impacts due to a strong earthquake occurring in the NMSZ. The NMSZ covers the Mississippi River basin from Illinois to eastern Arkansas and is known for a series of three strong earthquake sequences (with estimated magnitudes of M > 7) that occurred in 1811-1812

(Figure 5). The U.S. Geological Survey (USGS) estimates a 25% - 40% probability of having an earthquake in the NMSZ with a magnitude 6 or larger in the next 50 years, and a 7% - 10% probability of an event similar to one of the 1811–1812 sequences in the same time period (Petersen et al., 2015). The SASZ, which extends into Alabama, is primarily responsible for the low-level seismicity and periodic small earthquakes, with occasional minor damage (Figure 5). It extends from West Virginia into central Alabama, following the Appalachian Mountain chain. The SASZ is an intraplate seismic zone and is considered to be one of the most active earthquake zones in the eastern U.S. (Steigert, 1982). Seismicity in the SASZ is related to crustal uplift and compression, which in turn, is thought to reactivate ancient faults that developed during orogenic events associated with "Wilson" cycles of supercontinent amalgamation and break-up (Wilson, 1966; Hatcher, 1987; Thomas, 2006).

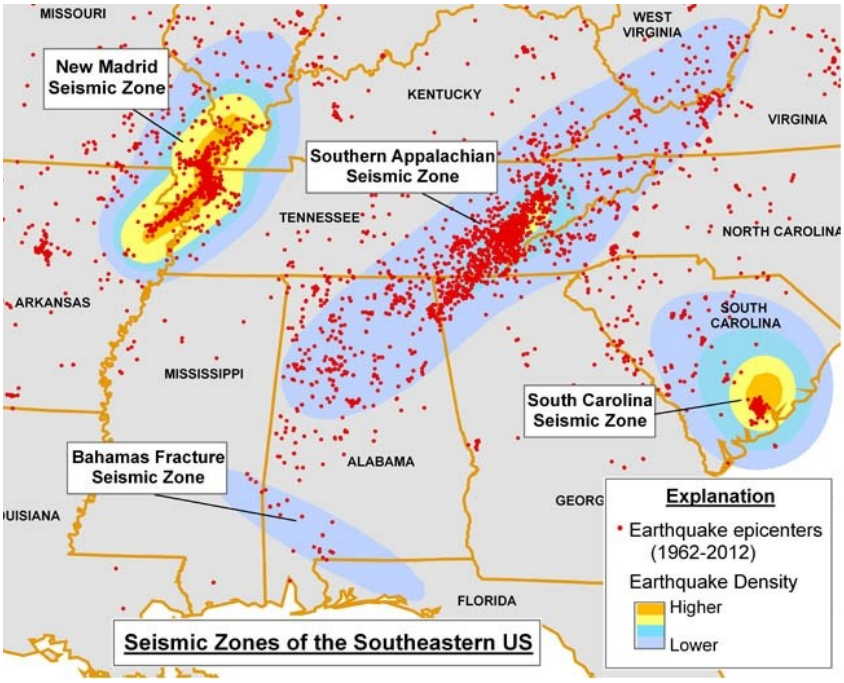

Figure 5. Seismic Zones of the Southeastern U.S. The Southern Appalachian Seismic Zone is located in the southwestern section of the NE-trending Appalachian Mountain belt, which extends from Virginia to Alabama. (from https://gsa.state.al.us/)

Historically, earthquakes have been recorded throughout all parts of Alabama. The USGS maintains an earthquake database dating back to 1973, although the catalog is complete to M ≥ 2 only in regions with a contributing local seismic network (http://earthquake.usgs.gov/earthquakes/search). A more complete catalog (M ≥ 3) dating back to 1568 can be downloaded at https://github.com/usgs/nshmp-haz-catalogs, which was used to develop the 2014 National Seismic Hazard Map (Petersen et al., 2015). Seismic records from 1886 show 310 earthquakes with epicenters in north Alabama, although recent seismicity based on better network coverage and lower detection thresholds suggests that this number may be much higher (Figure 6).

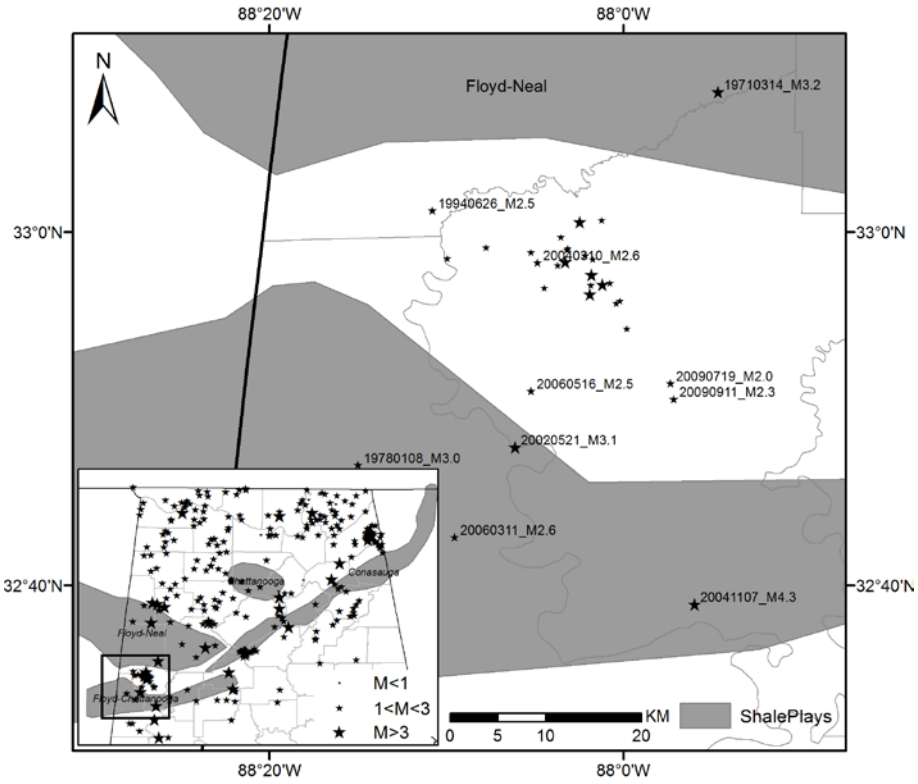

Figure 6. Historical seismicity around Greene County, Alabama. Epicenters of earthquakes in the Greene County cluster are represented by different sized stars. Labeled stars show the locations for earthquake epicenters before the cluster, with the date and magnitude in the label. Insert map shows the regional seismicity in north and central Alabama. Earthquake epicenters are represented by different sized stars. (from https://www.eia.gov/)

The recorded history shows that most of the earthquakes recorded in Alabama have been small to moderate, with magnitudes between 1 and 3. The more notable recorded earthquakes, however, include the 1986 M 4.5 Tuscaloosa earthquake, 1997 M 4.9 Escambia earthquake (Gomberg and Wolf, 1999), 2001 M 3.9 Pleasant Grove earthquake east of Huntsville, and the 2003 M 4.9 Fort Payne earthquake in northeastern Alabama. Although most of the earthquakes occurring in the state are shallow, a 15-km depth was estimated for the Fort Payne event. Both the Escambia and Fort Payne events caused some minor ground failure and structural damage. The Fort Payne earthquake also caused a shutdown of the underground water supply for the town of Valley Head, Alabama. Prior to the onset of the recent Greene County cluster, the historical record contains only 10 earthquakes recorded in the Greene County area (Table 1).

Table 1. Historical seismicity in Greene County area.

No.	Origin Time	Latitude	Longitude	Depth(km)	Magnitude
1	1971-03-14T17:27:00	33.132	-87.911	10	3.2
2	1978-01-08T11:34:00	32.780	-88.250	5	3.0
3	1994-06-26T05:50:00	33.020	-88.180	8.7	2.5
4	2002-05-21T20:35:34	32.797	-88.102	5	3.1
5	2004-03-10T03:06:48	32.971	-88.081	0	2.6
6	2004-11-07T11:20:21	32.649	-87.933	5	4.3
7	2006-03-11T08:08:54	32.712	-88.159	30.7	2.6
8	2006-05-16T05:23:19	32.850	-88.087	20.5	2.5
9	2009-07-19T00:00:00	32.857	-87.956	0	2.0
10	2009-09-11T16:23:58	32.842	-87.953	0.63	2.3

Data and processing

It is a complicated and time-intensive process to evaluate causation for the clustered seismicity. In order to investigate the source of clustered seismicity in Greene County, Alabama, this study follows a sequence of steps: (1) obtain the waveform data of earthquakes identified through a catalog search of Incorporation Research Institutions for Seismology (IRIS) and National Earthquake Information Center (NEIC) databases; (2) use the waveforms to relocate the earthquake hypocenters; (3) develop a set of master events for two closest stations (NM.EUAL, N4.Z47B) with which to search continuous waveform data to identify additional earthquakes; (4) conduct focal mechanism analyses for earthquakes ≥ M 3.0 using broadband waveforms and moment tensor inversion; and (5) analyze the resulting information in the context of geologic information and well injection records to determine the likely sources of the earthquake clusters.

Data collection

Table 2 lists the origin time, location, depth, and magnitudes of the largest earthquakes in the Greene County swarm occurring from November 2014 through September 2016 (http://earthquake.usgs.gov/earthquakes/). Although many smaller earthquakes have occurred, they are not routinely located. The corresponding waveform data for these 21 events were downloaded from the IRIS database (http://www.iris.edu/) for the stations shown in Figure 7. To avoid spatial biasing, 25 three-component, high-gain broadband seismic stations were selected to achieve full azimuthal coverage. Waveform data from the IRIS database were archived at 100

samples per second. The data for each earthquake were filtered with a bandpass of 0.1 Hz to 10 Hz and instrument responses were removed.

Table 2. Earthquakes for the northwestern Greene County from November 2014 to September 2016.

No.	Origin Time	Magnitude	Latitude	Longitude	Depth(km)
1	2014-11-20T10:25:31	3.80	32.9411	-88.0317	5.00
2	2014-12-17T19:38:15	3.40	32.9504	-88.0198	9.17
3	2015-01-22T10:01:23	2.70	33.0110	-88.0207	2.89
4	2015-02-19T18:19:09	3.00	32.9083	-87.9971	4.63
5	2015-02-19T21:22:35	2.41	32.9840	-88.0527	0.02
6	2015-02-19T21:29:43	3.00	32.9497	-88.0307	2.95
7	2015-02-22T00:08:19	2.36	32.9683	-88.0620	0.00
8	2015-02-27T22:40:50	3.20	33.0093	-88.0412	19.58
9	2015-03-12T01:19:20	3.10	32.9718	-88.0550	0.00
10	2015-05-21T22:25:47	2.32	32.9470	-88.0745	7.95
11	2015-05-23T07:12:22	2.06	32.9740	-88.0288	4.56
12	2015-05-30T16:48:17	1.52	32.9848	-88.1293	0.20
13	2015-05-31T01:33:35	1.77	32.9772	-88.0363	0.22
14	2015-06-06T18:09:35	3.00	32.9347	-88.0034	5.75
15	2015-06-17T05:19:54	2.12	32.9828	-88.0533	0.00
16	2015-06-30T03:02:19	2.11	32.9948	-88.0590	0.01
17	2015-06-30T06:44:07	3.50	32.9594	-88.0301	5.00
18	2015-07-04T10:28:46	1.51	32.9745	-88.1660	4.69
19	2015-08-13T19:37:47	2.34	32.9515	-88.0128	0.61
20	2016-02-04T01:33:41	2.29	32.9325	-88.0068	0.01
21	2016-09-05T08:28:27	2.58	32.9802	-88.0872	0.01

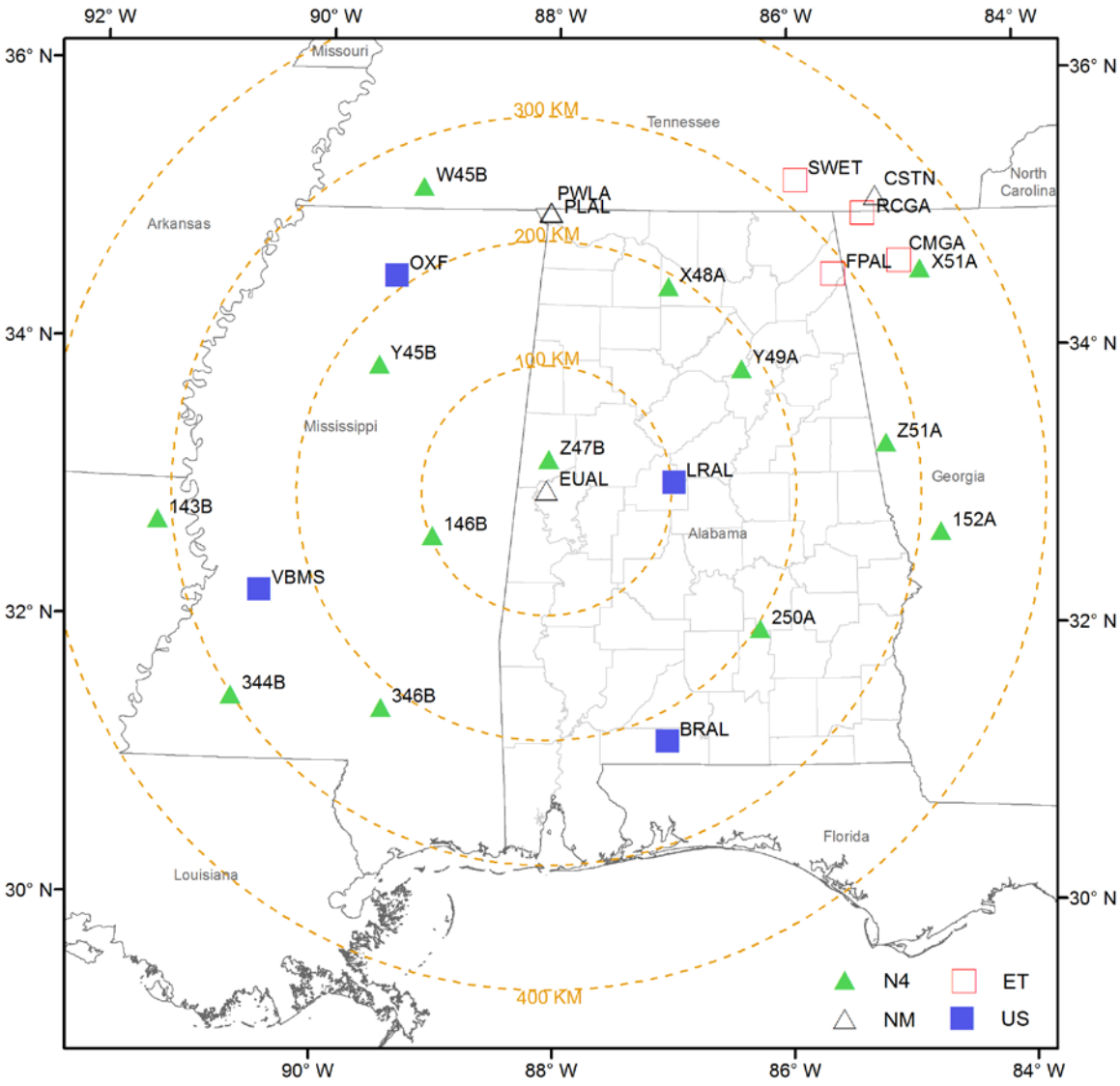

Figure 7. Regional seismic stations located within 400-km around the Greene County swarm. Green triangles represent stations in Central and Eastern US Network (N4), empty triangles represent stations in Cooperative New Madrid Seismic Network (NM), blue squares represent stations in United States National Seismic Network (US), and empty squares represent stations in CERI Southern Appalachian Seismic Network (ET). Yellow dashed circles give the distance from the Greene County epicentral area. (from http://www.fdsn.org/networks/)

Earthquake relocation

Evaluating the spatial pattern of the earthquake swarm requires reasonably precise and accurate locations of earthquake hypocenters. The epicentral uncertainty for the initial locations ranges from ~5 to 10 km, and depth uncertainty is about 10 km for most earthquakes less than M 3.0 (Frankel, 1995). The location uncertainty is a function of the number of seismic station records used, the spatial separation of stations, and the velocity models assumed. Regional velocity models often do not reflect local variability in geology. Depths are particularly problematic for some events, for which a default value of 5 km is typically assigned for shallow events. To reduce location uncertainties, a temporary seismic station (EUAL) was deployed from March 31 to September 23, 2015, by the Center for Earthquake Research and Information (CERI) at the University of Memphis. Archived continuous waveform data available from June 6 to September 23, 2015, are used in this study.

The station network assembled for this study provides good coverage around the Greene County swarm for relocating earthquakes and calculating fault plane solutions. The 1D velocity model shown in Table 3 was used to relocate the hypocenters. The velocity model represents a linear interpolation between center points of a block velocity model derived from a new global crustal model at 1×1 degrees – CRUST 1.0 (Laske et al., 2013).

Table 3. Velocity model used for earthquake relocation.

Layer	Thickness (km)	v_p (km/s)	v_s (km/s)	ρ (g/cm^3)
1	1.0	2.50	1.45	2.20
2	4.0	4.60	2.66	2.62
3	1.0	5.00	2.89	2.70
4	11.0	6.10	3.53	2.92
5	12.0	6.50	3.76	3.00
6	10.0	6.90	3.99	3.08
7	-	8.00	4.62	3.30

Two methods for relocating the earthquakes were used for this study (Figure 8). The first, Hypoinverse2000 (Klein, 2002), was used to relocate the earthquakes using the waveforms collected from the regional station network for known events. The program uses the arrival times of earthquake phases (e.g., P and S phases) to determine hypocentral locations. Arrival times of P and S waves for 18 template events ($M \geq 2$) with exceptionally clear phase arrivals were manually picked and the hypocentral locations recomputed using the velocity model shown in Table 3. The resulting event locations contain errors due to un-modeled variation in velocity structure.

To reduce the distortion in locations caused by deviations from the 1D velocity model, a double-difference relocation technique, HypoDD (Waldhauser and Ellsworth, 2000; Waldhauser, 2001), was used to further refine the relative locations of hypocenters within clusters (Figure 8). The double-difference algorithm attempts to minimize residual travel-time differences, or double differences, for a pair of earthquakes at a single station. The algorithm requires that the difference between two events be small compared to the distance between the hypocenters of the earthquakes and a station. In that case, the travel-time difference between the two events at a single station is approximately independent of un-modeled velocity heterogeneity along the ray paths between paired events at each station. The program HypoDD (Waldhauser, 2001) was used to identify and group clusters of earthquakes and then derive relative relocations within these clusters. It has been shown that the resulting locations can greatly improve the image of seismogenic features in situations where adequate data are available (Waldhauser and Ellsworth, 2000). Horizontal and depth errors in earthquake locations resulting from HypoDD were reduced to ~1.0 km.

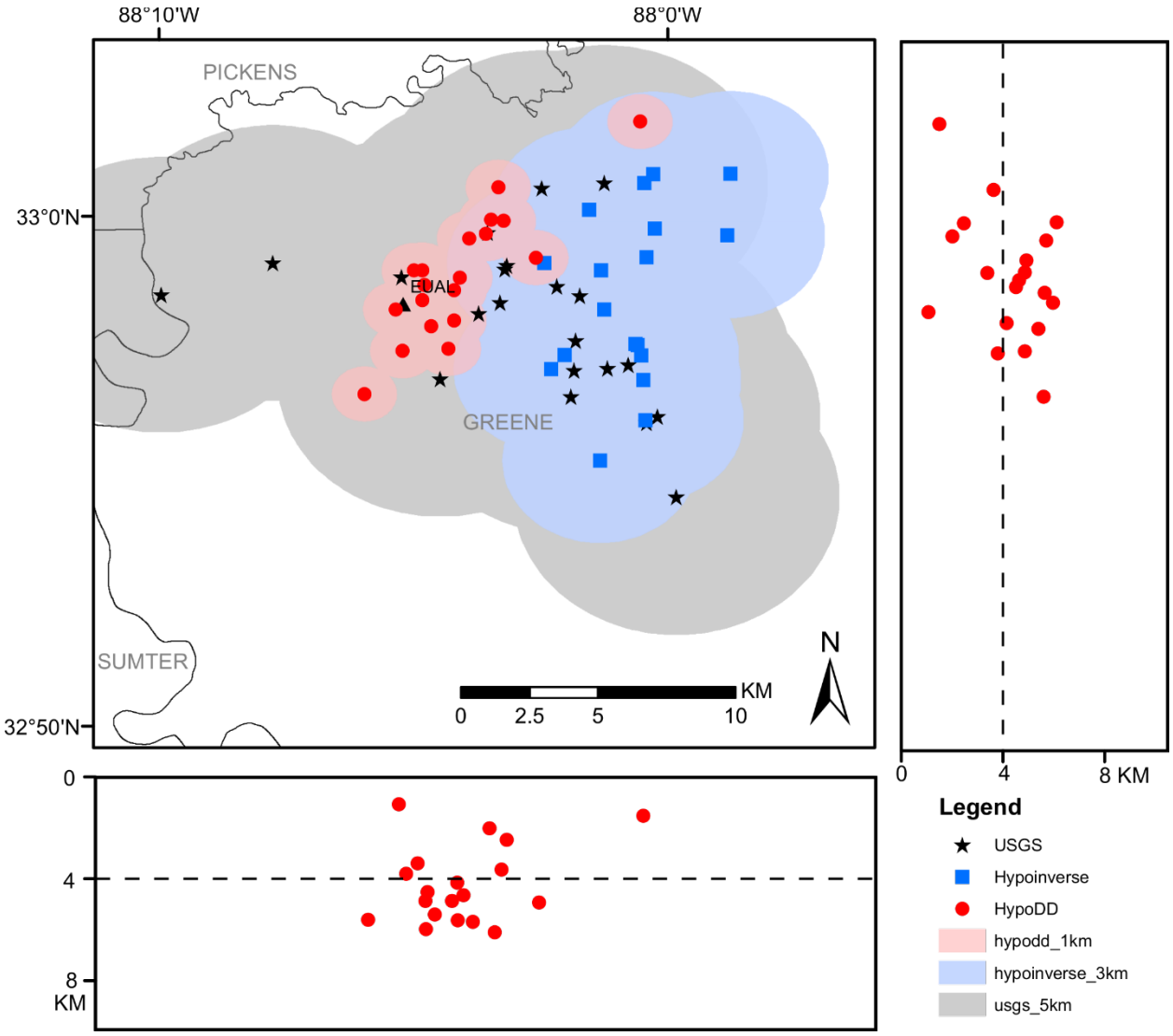

Figure 8. Earthquake relocation result for Greene County cluster. Black stars show the initial locations from USGS, blue squares show the relocated locations given by hypoinverse2000, and red dots show the final locations from HypoDD. Colored areas mark the average location uncertainties for HypoDD, Hypoinverse, and the original USGS locations. Cross sections show the depth variation of hypocenters projected into a vertical plane derived from HypoDD and dashed lines give the average depth.

Earthquake detection

Repeating earthquakes that have similar waveforms are assumed to originate from the same source and share the same propagation path. If the source of a particular waveform (usually with a large magnitude) can be determined, small earthquakes with similar waveforms can be located even if they are recorded by only a few stations. Here the sources are not considered as point sources, but rather faults with finite dimensions that can include seismogenic asperities or barriers. Because the number of seismic events increases exponentially with decreasing magnitude, target detection levels can be sufficiently low to allow detection of a sufficient number of events to illuminate active geologic features. For example, if an M 3.0 event has been detected by the national seismic array, there may be 10 or more M 2.0 and 100 or more M 1.0 events associated with this sequence. In this case, a local array designed to detect and locate M 1.0 events is likely to see enough seismic activity to assist with an interpretation of the causative structure.

In this study, the continuous waveforms recorded by two closest stations (NM.EUAL, N4.Z47B) were analyzed to identify additional earthquakes. Instead of using the classical detector – matched filter, which correlates a single template waveform with a continuous data stream to detect similar events, a subspace detector was constructed because repeating sources frequently produce varied waveforms not well represented by a single template. For each station used, subspace templates were created to search the available continuous waveform data to identify additional earthquakes observations. The search was performed using the subspace method of Chambers et al. (2015).

Detex (https://github.com/d-chambers/Detex) is an open source Python package for performing waveform similarity clustering and subspace detection. The main goal of such analyses is to determine if a group of seismic events are similar, meaning they have comparable source mechanisms and hypocenters, and to use such information to identify small, often difficult to detect, earthquakes. The method is described below.

Required files and data acquisition

There are two required files for Detex: the station key and the template key. The station key specifies station location, elevation, channels, start and cutoff time for continuous waveforms (Table 4). The template key contains information on each of the events that will be used to scan the continuous data for previously undetected events. Here, 18 initially located earthquakes with magnitude larger than 2.0 were selected as template earthquakes (Table 5). Detex can use a variety of data sources. Seismic data were downloaded through Obspy's fdsn module from IRIS and stored in a local directory structure for quick access. Seismic traces from three components of each station are multiplexed to form a single trace that includes all observable phases.

Table 4. Station key input used for subspace detection.

Network	Station	Starttime	Endtime	Lat (°)	Lon (°)	Elevation (m)	Channels
N4	Z47B	2015-06-30T00-00-00	2015-06-30T23-00-00	33.1989	-88.0696	64	HHZ-HHN-HHE
NM	EUAL	2015-06-30T00-00-00	2015-06-30T23-00-00	32.9714	-88.0867	76	HHZ-HHN-HHE

Table 5. Template key input used for subspace detection (for temporarily deployed station EUAL, only 4 events were recorded during three months).

Temid (Z47B)	Temid (EUAL)	Origin Time	Lat (°)	Lon (°)	Depth (km)	Mag
0	-	2014-11-20T10-25-31	32.9411	-88.0317	5	3.8
1	-	2014-12-17T19-38-15	32.9504	-88.0198	9.2	3.4
2	-	2015-01-22T10-01-23	33.011	-88.0207	2.9	2.7
3	-	2015-02-19T18-19-09	32.9083	-87.9971	4.6	3
4	-	2015-02-19T21-22-35	32.984	-88.0526	0	2.4
5	-	2015-02-19T21-29-43	32.9497	-88.0307	3	3
6	-	2015-02-22T00-08-18	32.9568	-88.0456	0	2.2
7	-	2015-02-27T22-40-50	33.0093	-88.0412	19.6	3.2
8	-	2015-03-12T01-19-20	32.9368	-88.0667	10.8	3.1
9	-	2015-05-21T22-25-47	32.947	-88.0745	7.9	2.3
10	-	2015-05-23T07-12-22	32.9739	-88.0288	4.5	2.1
11	-	2015-06-06T18-09-35	32.9347	-88.0034	5.8	3
12	0	2015-06-17T05-19-54	32.9831	-88.0533	0	2.1
13	1	2015-06-30T03-02-19	32.9948	-88.059	0	2.1
14	2	2015-06-30T06-44-07	32.9594	-88.0301	5	3.5
15	3	2015-08-13T19-37-47	32.9515	-88.0128	0.6	2.3
16	-	2016-02-04T01-33-41	32.9325	-88.0068	0	2.3
17	-	2016-09-05T08-28-27	32.9447	-88.185	5.5	2.6

Clustering

In order to have a very similar appearance at one or more stations, the earthquakes of a given cluster must have similar rupture mechanisms and similar paths to each station, which means that their hypocenters should cluster together. To form waveform similarity groupings on each station, multiplexed waveform of every event was cross-correlated with every other event, by which similarity matrices are created independently for each station (Figure 9). A single link hierarchical clustering algorithm was used to perform the clustering up to a determined dissimilarity level (Figures 10 and 11). At the same time, a clusterStream object is created, which is essentially a container for groupings on each station. The main input parameter is the required correlation coefficient, it was set as 0.6, below which clustering would not occur. Although

several correlation coefficients were tested, this value yielded the most reasonable results. Once the clusters are identified, they are used to construct the subspace detector described below.

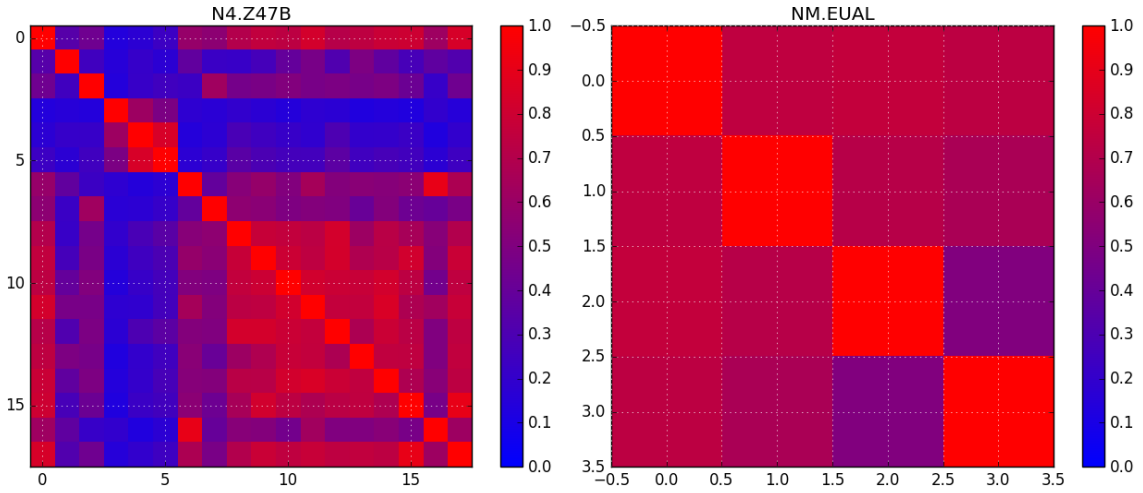

Figure 9. Similarity matricies on each station (N4.Z47B and NM.EUAL); axes represent template ID (Temid) and colored squares represent similarity related to correlation coefficient for individual pairs.

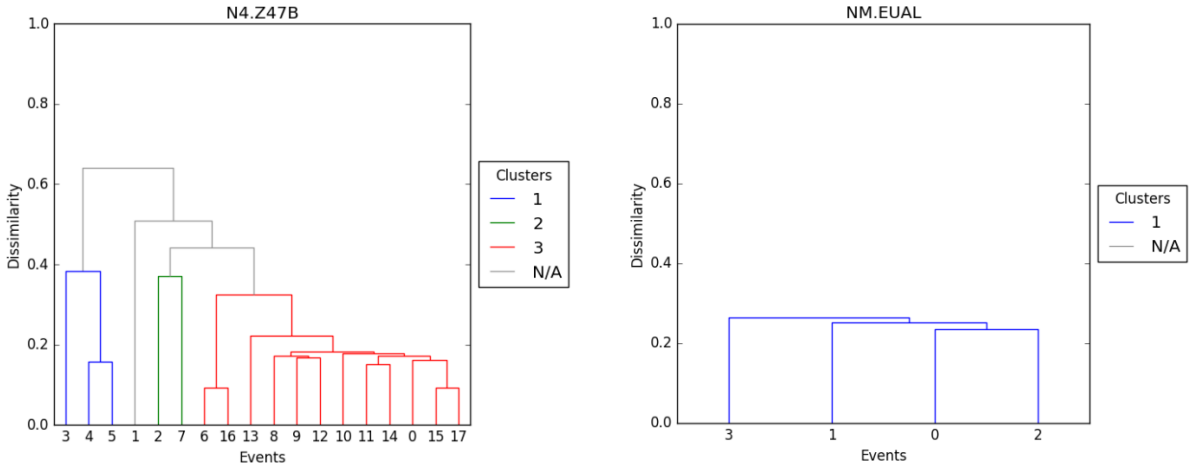

Figure 10. Dendrogram created to visualize grouping structure on each station, horizontal axis represents template ID (Temid) and vertical axis represents dissimilarity related to correlation coefficient.

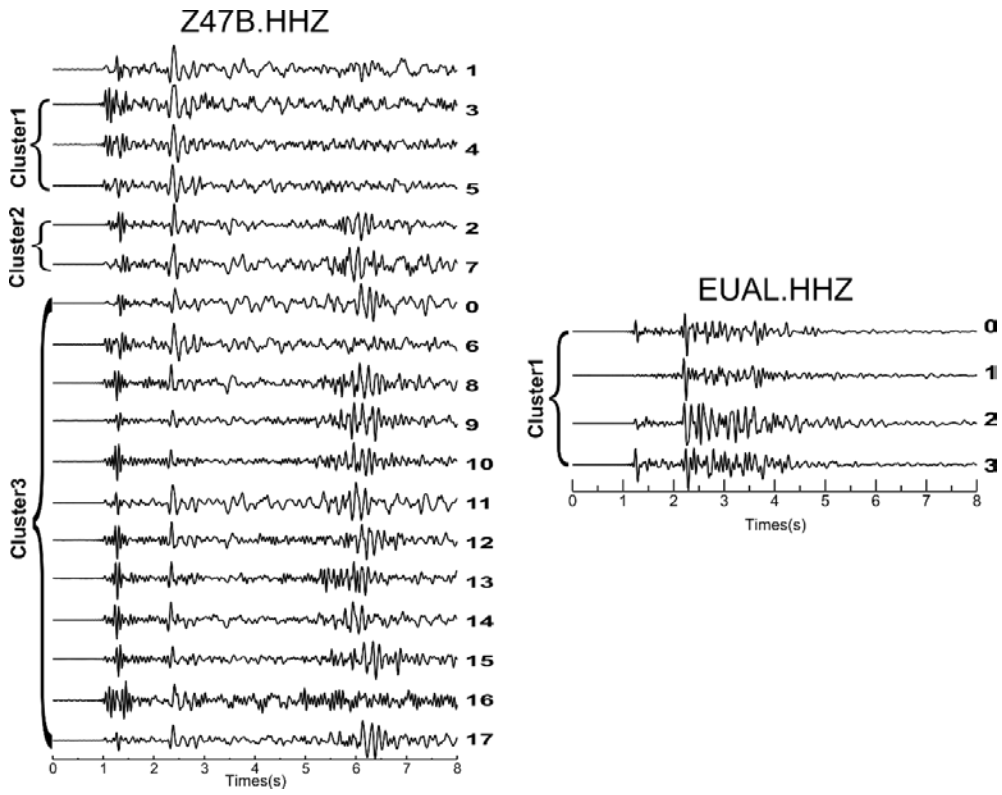

Figure 11. Vertical components waveforms of template earthquakes on station EUAL and Z47B.

Subspace detection

The subspace creation process was applied to each cluster, or waveform similarity group. The process involves: (1) aligning the waveforms to optimize similarity, where the waveforms are aligned and trimmed to a length of 30s starting from a user-defined pick time (ideally the first arrival); (2) performing a singular value decomposition to calculate an orthonormal basis that spans the training events; (3) determining a required dimension of representation, the fewest dimensions of representation are calculated based on the fractional energy capture of 90%; and (4) setting a significant detection statistic threshold. As a final step, (5) the subspace detectors are run on each station and a detection is declared whenever any subspace's threshold is

exceeded. The results are saved to a SQLite database. A more detailed description of those steps above can be found in Chambers et al. (2015).

The subspace detection technique identified 42 additional microearthquakes with clear arrivals at station EUAL and Z47B from three months of continuous data. The magnitudes of these detected earthquakes range from M 0.5 to M 2, and often, first arrivals could not be picked, which makes the location calculation difficult. The number of detected earthquakes represent a nearly 10-fold increase from the 5 template events within the same three months period. This result suggests that many more earthquakes were occurring than were reported in the earthquake catalog. The waveform cross section from Figure 12 illustrates the repeating characteristics of the Greene County swarm.

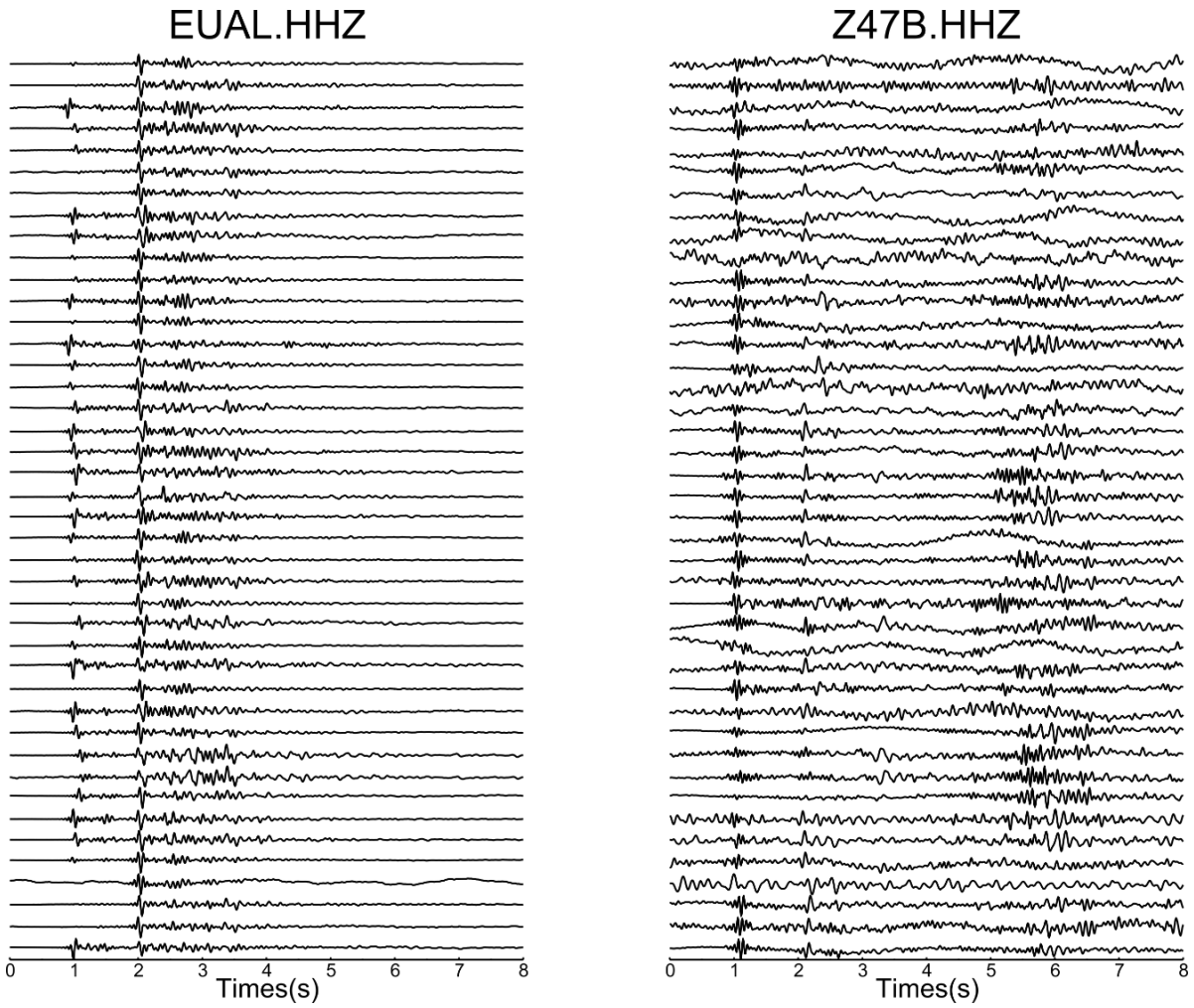

Figure 12. Vertical component waveforms of detected earthquakes on station EUAL and Z47B. Similarity among traces indicates a source is repeatedly ruptured.

Focal mechanism analysis

Focal mechanisms are important for understanding physics of individual earthquakes, and for studying seismotectonics of a region; they also serve as a basic input for seismic hazard assessment. From the 21 located earthquakes (Table 2) in northwestern Greene County, eight earthquakes with M > 3 were selected for the focal mechanism analysis, in addition to the two largest events for which focal mechanisms had been reported by NEIC.

Because the magnitudes are small and onset polarities can be hard to pick on all but the closest stations, a point source approximation and the moment tensor (MT) are used to get the focal mechanism for each earthquake. MT determination using broadband waveforms is a non-linear inverse problem. Waveforms recorded at a seismic station, $W(t)$, are composed of three elements: $W(t) = S(t) * G(t) * I(t)$, where $S(t)$ represents the source, $G(t)$ stands for the Green's functions, and $I(t)$ is the instrument response. Therefore, retrieving source parameters of one earthquake $S(t)$ requires deconvolving instrument response $I(t)$ and Green's functions $G(t)$ from the actual data $W(t)$. The instrument responses were removed when obtaining the waveform data. The waveform data is expressed in displacement or in velocity: $u(t) = S(t) * G(t)$. The corresponding synthetic displacement $u(t)$ for a douple-couple source can be expressed as: $u(t) = M_0 \sum A_i(\theta - \varphi, \delta, \lambda) G_i(t)$, where G_i are the Green's functions, A_i are the radiation coefficients, θ is the station azimuth, M_0 is scalar moment, and φ, δ, and λ are strike, dip, and rake, respectively. A grid search is performed in all possible solutions of strike ($0^\circ \leq \varphi \leq 360^\circ$), dip ($0^\circ \leq \delta \leq 90^\circ$), and rake ($-180^\circ \leq \lambda \leq 180^\circ$) to obtain the best fit by finding the minimal residual between the data and synthetics. This procedure consists of the following three steps: (1) computing Green's functions, (2) preparing data seismograms, and (3) deriving focal mechanism solutions. Here focal mechanism solutions are computed using the “Cut and Paste” method (CAP) (Zhu and Helmberger, 1996). This method decomposes seismograms and uses amplitude information in different time windows (e.g., Pnl [0.05 ~ 0.3 Hz] and surface wave [0.02 ~ 0.05 Hz]) to increase the stability and resolution of focal mechanism solution. Figure 13 is an example of focal mechanism analysis for one of the selected earthquakes with the MT

inversion method stated above. The focal mechanisms are used to constrain the relation of the earthquakes to geologic structure (see discussion below).

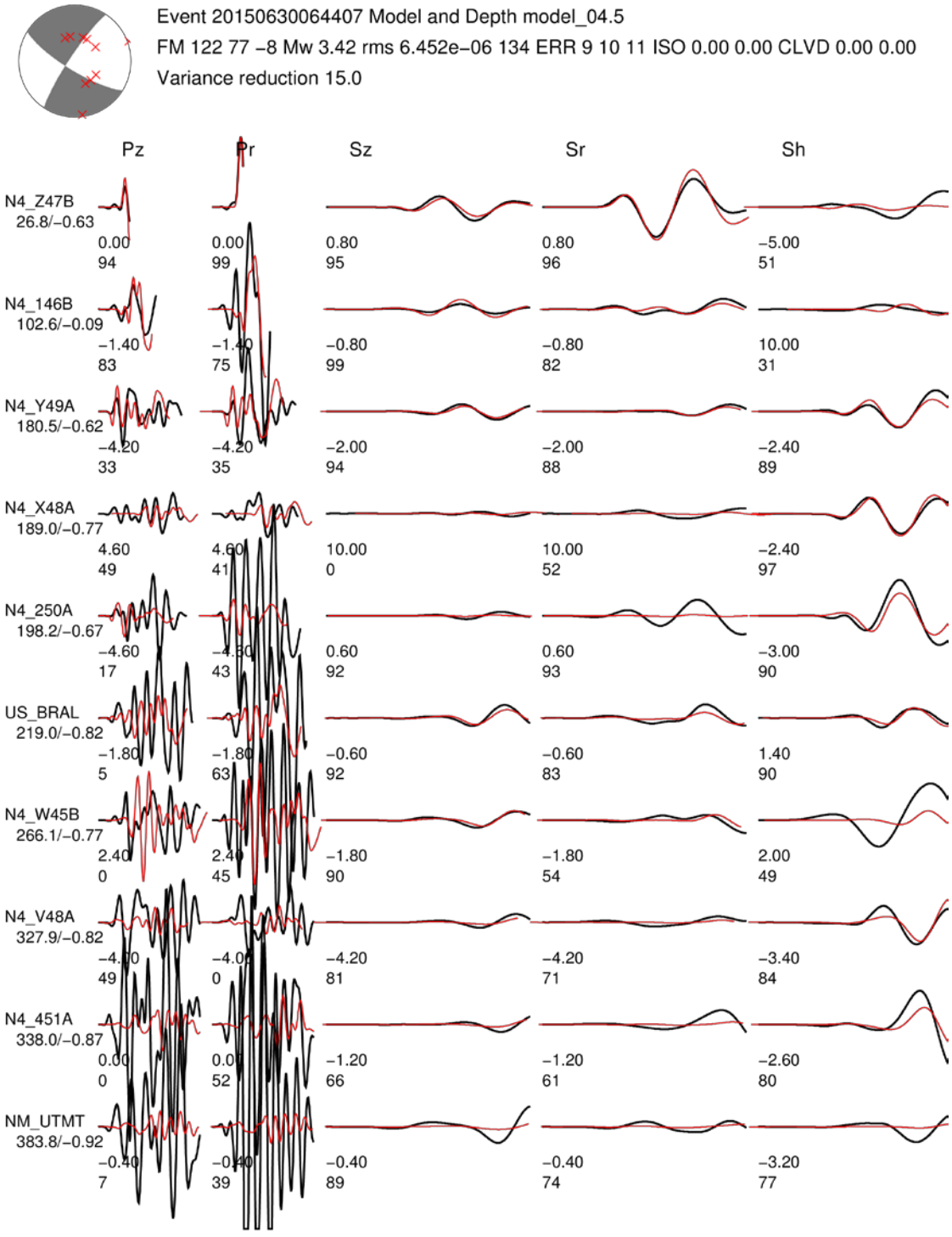

Figure 13. Comparison between synthetic (red) and observed (black) seismograms for moment tensor inversion. The numbers on the lower left side of the seismograms are the time shifts (upper) and cross-correlation coefficient in percent (lower). Positive time shifts mean delay or right-shift of the synthetic seismograms.

Discussion of possible sources

Induced seismicity has gained much attention over the past decade, as evidenced by the rise in recent scientific meetings and conferences focused on this subject. Although the basic mechanism of induced earthquakes is well understood, each case is a product of the local geology, including faulting, in-situ stress conditions, hydrology, and the characteristics of the causative source (Davies et al., 2013). The vast majority of earthquakes are tectonic (naturally occurring), but under some circumstances human activities can trigger seismicity. Induced seismic activity has been attributed to a broad range of human activities, including underground injection (Ellsworth, 2013), oil and gas extraction (Friberg et al., 2014; Davies et al., 2013), impoundment of large reservoirs behind dams (Gupta, 1992), geothermal projects (Deichmann and Giardini, 2009), mining extraction (Chambers et al., 2015), quarrying operations (Seeber et al., 1998), underground nuclear tests (Hamilton et al., 1972), and sinkhole formation (Navak and Dreger, 2014).

Figure 14 depicts the locations for sinkholes (Geological Survey of Alabama, https://gsa.state.al.us/), mines (Alabama Surface Mining Commission, http://www.surface-mining.state.al.us/), sand pits, and quarries (Stone Quarries and Beyond, http://quarriesandbeyond.org) in west-central Alabama around Greene County. There are no mines and quarries located within 50 km of the Greene County epicentral cluster, and no sand pits within Greene County. Although there are sinkholes nearby the epicentral area, the number

is not consistent with the number of earthquakes recorded. In addition, most of the earthquakes are too large for sinkhole collapse to be a reasonable explanation.

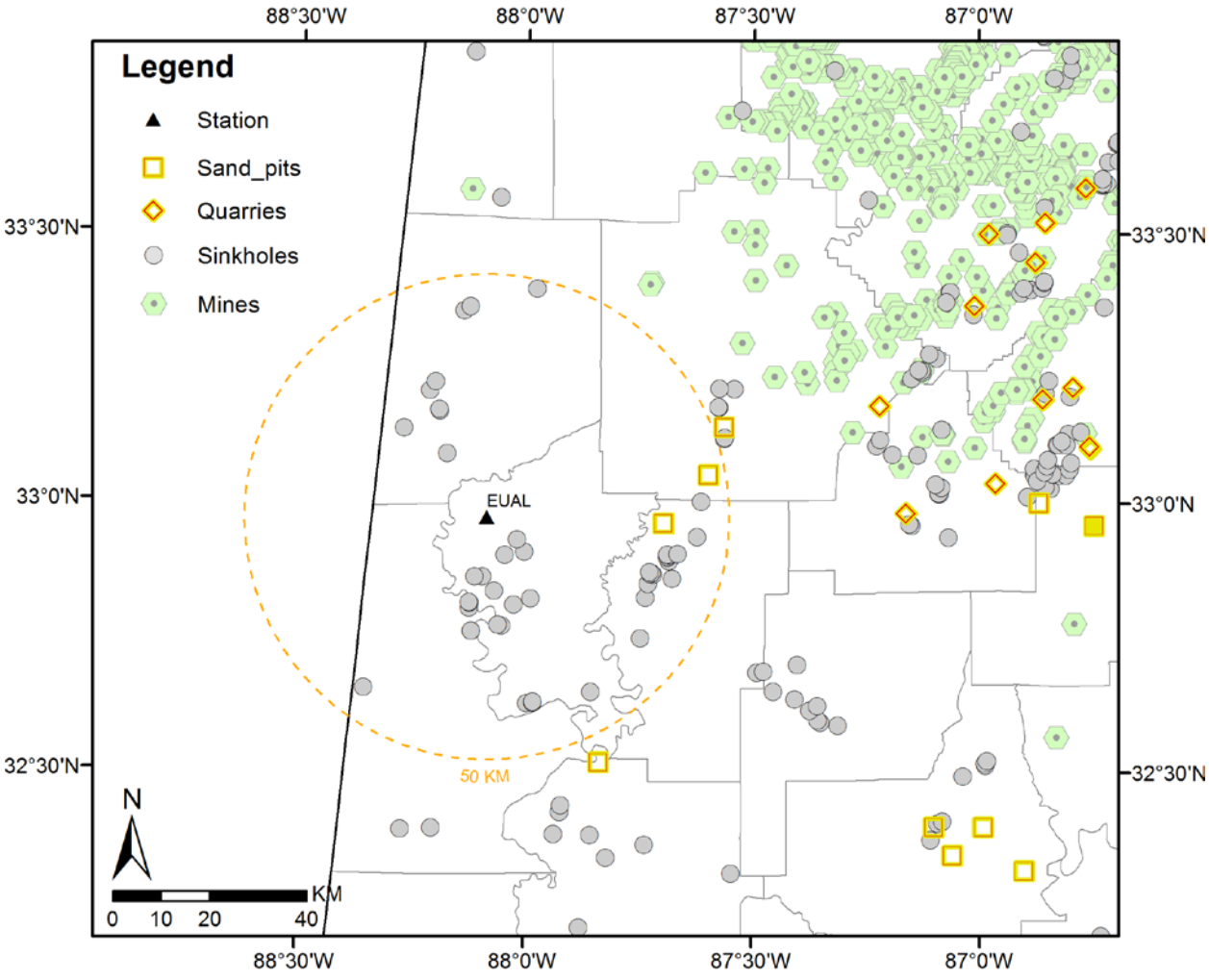

Figure 14. Mines (http://www.surface-mining.state.al.us/), quarries and sand pits (http://quarriesandbeyond.org), and sinkholes (https://gsa.state.al.us/) in west-central Alabama. Yellow dashed circle indicates the 50 km distance from the Greene County epicentral cluster.

The Greene County cluster is located within the BWB where natural gas was first extracted in the 1970s and thousands of hydraulic fracturing natural gas wells have been operating since 1999 (Hall and Bolin, 2009). The BWB remains a target of regional oil and gas drilling today. Although public concern has focused on hydraulic fracturing as a major source of induced seismicity, many scientists suggest that hydraulic fracturing has a far lower potential to induce earthquakes than underground salt-water disposal. Rubinstein and Mahani (2015) conclude that (1) fracturing operations are intended to fracture the rock, whereas injection operations are intended to dispose waste water into permeable layers; (2) fracturing typically lasts several days, whereas injection may last years, so the total energy put into the formation during fracturing is relatively small; (3) fluids in a fracture treatment are largely stored in the fractures, whereas the fluid from injection is stored in porous and permeable rock formations; and (4) unlike disposal well operations, hydraulic fracturing operations followed by production operations generally result in lowering of reservoir pore pressure in proximity to the well.

The majority of disposal wells in the United States do not pose a hazard for induced seismicity, but under some geologic and reservoir conditions a limited number of injection wells have been responsible for induced earthquakes (Dieterich et al., 2015). Figure 15 illustrates the oil and gas wells in the BWB (State Oil and Gas Board of Alabama, https://www.gsa.state.al.us/ogb/wells). Within 15 km from the Greene County epicentral area, there are a few dry and abandoned undesignated wells (labeled as UN). The class type of "Undesignated" refers to test wells or wells drilled for stratigraphic information only. The three nearest active salt-water disposal wells, Dorroh #32-12-SWD 1 (8864-SWD-90-9), Cork SWD 3-14 #1 (8467-SWD-90-5), and Shirley 22-1-SWD #2 (9976-SWD-91-4), are located in the

southwest corner of Tuscaloosa County. Although these three wells have been inactive for several years, they remain kept as back-up for water disposal for the Robinson Bend Coal Degassification field. The operator, Castleton Commodities International LLC, currently discharges their produced water and periodically injects small amounts of water (tens of barrels periodically over several months) to keep the Class II UIC permit active (B. Gregory, personal communication, 2016).

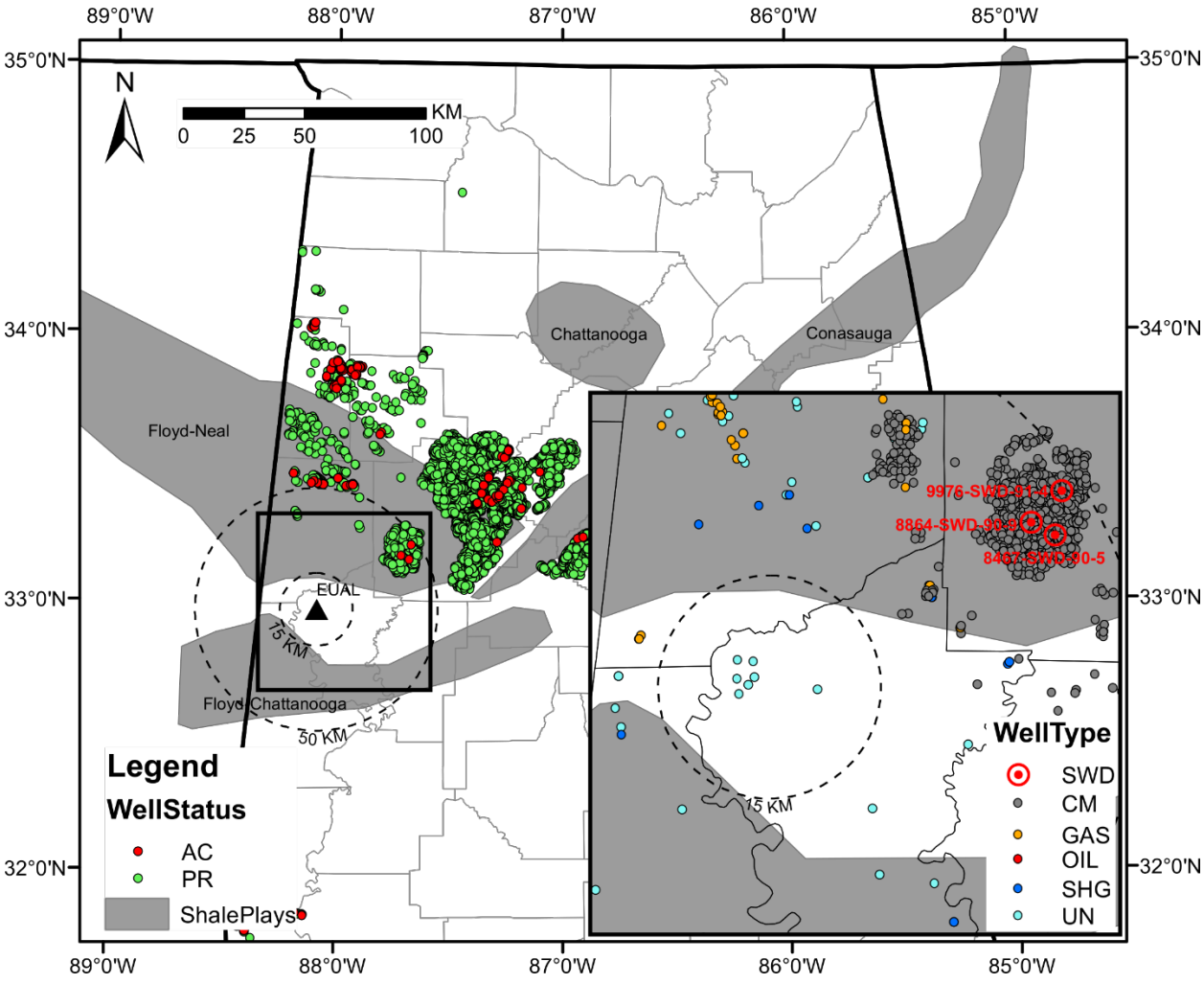

Figure 15. Oil and Gas wells in north and central Alabama. Dashed circles indicate the 15 & 50 km distance from the Greene County cluster epicenter. Inserted map shows the enlarged area within the red rectangle. (Well status: AC – Active, PR – Producing. Well type: CM - Coal Bed Methane, GAS - Natural Gas, OIL – Oil, SHG - Shale Gas, SWD - Salt Water Disposal, UN – Undesignated). See text for discussion. (https://gsa.state.al.us/)

The main physical mechanism responsible for injection-induced seismicity is the increased pore pressure on critically stressed fault surfaces, which decreases the effective normal stress and effectively unclamps the fault, allowing it to slip (Hubbert and Rubey, 1959; Ellsworth, 2013). Stress can accumulate in the earth's crust through natural tectonic processes and can be stored for millennia before being released in an earthquake sequence (Zoback and Gorelick, 2012). The largest earthquakes thought to be injection-induced have occurred mostly in Precambrian basement rock, where the rock is sufficiently strong to store larger amounts of tectonic strain energy. Induced seismicity usually is confined to the shallow (< 10.0 km) part of the earth's crust, often initiating in the vicinity of the formation where the injection is occurring. For example, the 2011 Youngstown, Ohio, earthquakes (maximum event M 4.0) occurred at depths of ~ 4.0 km in the Precambrian basement (Kim, 2013), and the majority of potentially induced earthquakes in Oklahoma have occurred at depths of ~ 6.0 km in the shallow crystalline basement (McNamara et al., 2015). These shallow depths explain why induced earthquakes as small as M 2.0 can be felt. For the Greene County cluster, the average depths of the earthquakes are around 4.0 km (Figure 8), from both the USGS catalog and this study's relocation results.

Earthquakes within 15 km of an active injection well, which is based upon the sum of a 5-km induced radius (Davis and Frohlich, 1993) and 10-km estimate of earthquake epicenter location (Frankel, 1995), are considered to be associated with that well (Weingarten et al., 2015). Although a mechanism related to well injection for the Greene County cluster cannot be unequivocally ruled out, the long distance (~ 40 km) between the epicentral area and the nearest active salt-water disposal wells, along with the history of well injections suggest that salt-water injection is likely not the cause of the swarm. The closest producing coalbed methane wells are

similarly far (~ 35 km) from the center of the Greene County cluster. However, it is possible that a pore-pressure front could propagate along faults bordering the Precambrian graben from the active resource extraction areas located northeast of Greene County, causing critically stressed Precambrian basement (~ 6 km) faults to slip. The swarm area might also be hydrologically connected to the resource extraction area via the NNE- to NE-trending Precambrian basement faults (see Figure 16 and discussion below). Future work involving hydrologic modeling could address this possibility.

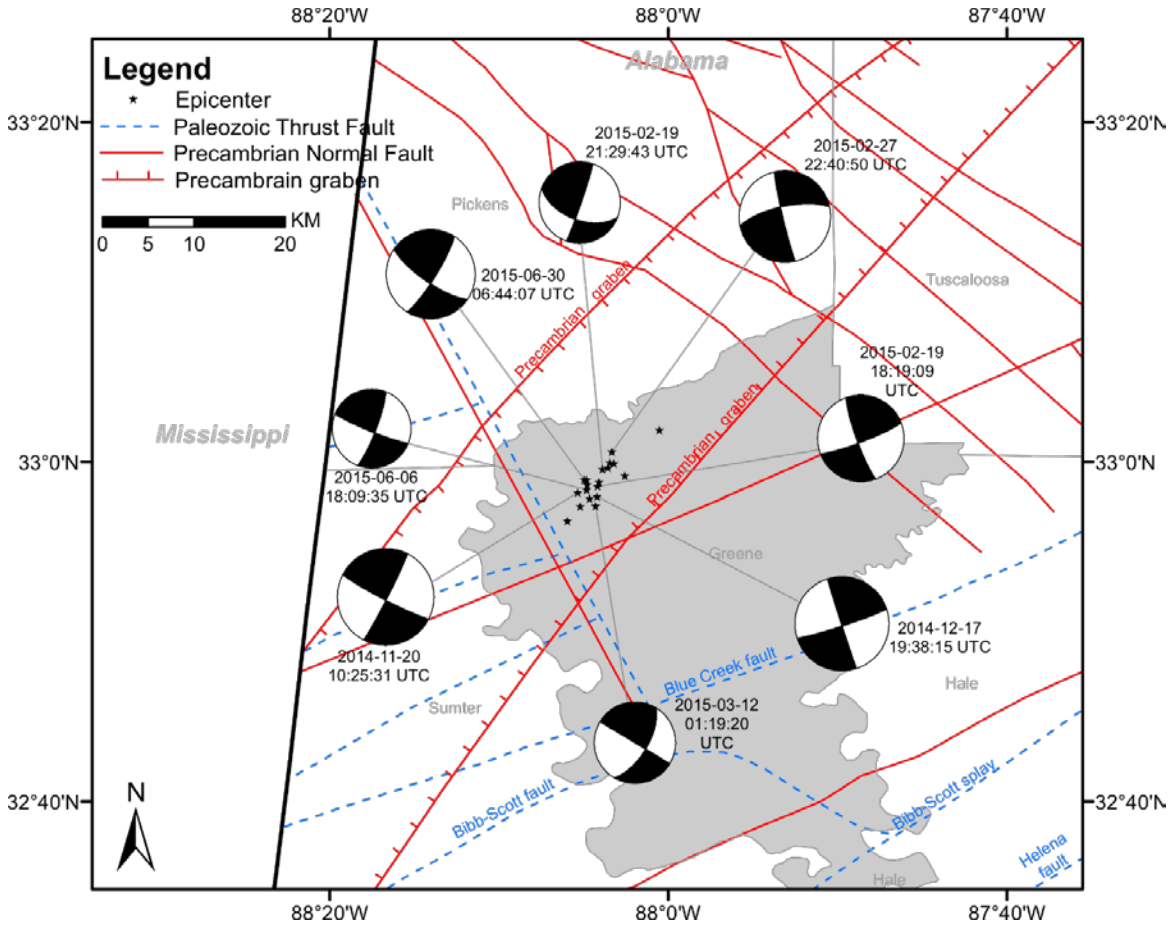

Figure 16. Preliminary focal mechanisms for the M > 3 events in Greene County swarm are shown. The focal mechanisms suggest right-lateral strike-slip motion on NE-oriented faults, or left-lateral strike-slip on NW-oriented faults. Labels of focal mechanisms indicate date of earthquake. Basement faults are shown with lines; red lines indicate Precambrian normal faults and blue dashed lines represent Paleozoic thrust faults. (https://gsa.state.al.us/)

Although recent research has demonstrated an unequivocal link between resource recovery processes and seismicity, regional tectonic processes and geologic structures are also responsible for seismic swarms. As seen in Figure 16, the relocated Greene County epicenters follow a northeast linear trend that is subparallel with the faults bounding the Precambrian graben. The exact location of basement faults is not, however, well constrained (W. Thomas, personal communication, 2016). Focal mechanisms calculated for earthquakes with M > 3.0 indicate either dextral motion on NNE- to NE-trending planes or sinistral motion on NNW- to NW-trending planes. The former possibility (i.e., NE-trending) aligns with the northeast-trending faults bounding the graben, whereas the latter orientation follows the northwesterly strike of a set of Paleozoic and Precambrian basement faults, some of which may be transform faults related to crustal rifting. Because the Greene County cluster follows a northeasterly trend, this study favors the interpretation that the earthquakes may represent a continuation or southwesterly migration of the SASZ. Powell et al. (1994) attributed the SASZ seismicity to strike-slip reactivation of an ancient fault system, because earthquake focal mechanisms consistently indicate dextral motion on NNE-trending planes and sinistral motion on east-trending planes. Their results are consistent with the geometry and kinematics inferred from this study. Steltenpohl et al. (2010) used the aeromagnetic data to constrain the southern termination of the New York - Alabama lineament and argued that the lineament reflects a crustal-scale, right-lateral strike-slip motion, an interpretation that fits the focal mechanism determined in this study. Taken together, the results suggest that current intraplate stresses in eastern North American may be concentrating seismicity along the Grenville province boundary into central Alabama. This possibility is

consistent with an interpretation put forward by Powell et al. (2016) for areas to the northeast along the Appalachian Mountain chain.

Conclusions

By conducting a spatiotemporal analysis using seismic data and geologic data, the results of this study reveal possible sources for the Greene County earthquake cluster from 2014 to 2016. Anthropogenic activities including underground injection, oil and gas extraction, mining extraction, quarrying operations, and sinkhole formation are likely not the cause of the swarm, even though they cannot be unequivocally ruled out. It is possible that a pore pressure front could propagate along faults associated with the Precambrian graben from the active resource extraction areas located northeast of Greene County, causing critically stressed Precambrian basement fault to slip. Calculated focal mechanisms indicate either dextral motion on NNE- to NE-trending planes or sinistral motion on NNW- to NW-trending planes and suggest the interpretation that the earthquakes may represent a continuation or southwesterly migration of the SASZ, which is consistent with previous investigations. Taken together, the results suggest that current intraplate stresses in eastern North American may be concentrating seismicity along the Grenville province boundary into central Alabama.

References

Bakun, W.H., Hopper, M.G., 2004. Magnitudes and Locations of the 1811–1812 New Madrid, Missouri, and the 1886 Charleston, South Carolina, Earthquakes. Bull. Seismol. Soc. Am. 94, 64–75. doi:10.1785/0120020122

Barnhart, W.D., Benz, H.M., Hayes, G.P., Rubinstein, J.L., Bergman, E., 2014. Seismological and geodetic constraints on the 2011 Mw5.3 Trinidad, Colorado earthquake and induced deformation in the Raton Basin. J. Geophys. Res. Solid Earth 119, 2014JB011227. doi:10.1002/2014JB011227

Chambers, D.J.A., Koper, K.D., Pankow, K.L., McCarter, M.K., 2015. Detecting and characterizing coal mine related seismicity in the Western U.S. using subspace methods. Geophys. J. Int. 203, 1388–1399. doi:10.1093/gji/ggv383

Davies, R., Foulger, G., Bindley, A., Styles, P., 2013. Induced seismicity and hydraulic fracturing for the recovery of hydrocarbons. Mar. Pet. Geol. 45, 171–185. doi:10.1016/j.marpetgeo.2013.03.016

Davis, S.D., Frohlich, C., 1993. Did (Or Will) Fluid Injection Cause Earthquakes? - Criteria for a Rational Assessment. Seismol. Res. Lett. 64, 207–224. doi:10.1785/gssrl.64.3-4.207

Deichmann, N., Giardini, D., 2009. Earthquakes Induced by the Stimulation of an Enhanced Geothermal System below Basel (Switzerland). Seismol. Res. Lett. 80, 784–798. doi:10.1785/gssrl.80.5.784

Dieterich, J.H., Richards-Dinger, K.B., Kroll, K.A., 2015. Modeling Injection-Induced Seismicity with the Physics-Based Earthquake Simulator RSQSim. Seismol. Res. Lett. 86, doi:10.1785/0220150057

Ellsworth, W.L., 2013. Injection-Induced Earthquakes. Science 341, 1225942. doi:10.1126/science.1225942

Frankel, A., 1995. Mapping Seismic Hazard in the Central and Eastern United States. Seismol. Res. Lett. 66, 8–21. doi:10.1785/gssrl.66.4.8

Friberg, P.A., Besana-Ostman, G.M., Dricker, I., 2014. Characterization of an Earthquake Sequence Triggered by Hydraulic Fracturing in Harrison County, Ohio. Seismol. Res. Lett. 85, 1295–1307. doi:10.1785/0220140127

Frohlich, C., Ellsworth, W., Brown, W.A., Brunt, M., Luetgert, J., MacDonald, T., Walter, S., 2014. The 17 May 2012 M4.8 earthquake near Timpson, East Texas: An event possibly

triggered by fluid injection. J. Geophys. Res. Solid Earth 119, 581–593. doi:10.1002/2013JB010755

Göbel, T., 2015. A comparison of seismicity rates and fluid-injection operations in Oklahoma and California: Implications for crustal stresses. Lead. Edge 34, 640–648. doi:10.1190/tle34060640.1

Gomberg, J., Wolf, L., 1999. Possible cause for an improbable earthquake: The 1997 Mw 4.9 southern Alabama earthquake and hydrocarbon recovery. Geology 27, 367–370. doi:10.1130/0091-7613(1999)027<0367:PCFAIE>2.3.CO;2

Gupta, H.K., 1992. Reservoir Induced Earthquakes. Elsevier.

Hall, D.R., Bolin, D.E., n.d. The Petroleum Industry in Alabama, 1999–2007, Oil and Gas Report 3u. Geological Survey of Alabama for the State Oil and Gas Board.

Hamilton, R.M., Smith, B.E., Fischer, F.G., Papanek, P.J., 1972. Earthquakes caused by underground nuclear explosions on Pahute Mesa, Nevada Test Site. Bull. Seismol. Soc. Am. 62, 1319–1341.

Hatch, J.R., Pawlewicz, M.J., 2007. Introduction to the Assessment of Undiscovered Oil and Gas Resources of the Black Warrior Basin Province of Alabama and Mississippi. Hatch Joseph R Pawlewicz MJ Compil. Geol. Assess. Undiscovered Oil Gas Resour. Black Warrior Basin Prov. Ala. Miss. US Geol. Surv. Digit. Data Ser. DDS–69–I 6.

Hatcher, R.D., 1987. Tectonics of the southern and central Appalachian internides. Annu. Rev. Earth Planet. Sci. 15, 337–362.

Healy, J.H., Rubey, W.W., Griggs, D.T., Raleigh, C.B., 1968. The Denver Earthquakes. Science 161, 1301–1310.

Herrmann, R.B., Park, S.-K., Wang, C.-Y., 1981. The denver earthquakes of 1967-1968. Bull. Seismol. Soc. Am. 71, 731–745.

Horton, S., 2012. Disposal of Hydrofracking Waste Fluid by Injection into Subsurface Aquifers Triggers Earthquake Swarm in Central Arkansas with Potential for Damaging Earthquake. Seismol. Res. Lett. 83, 250–260. doi:10.1785/gssrl.83.2.250

Hubbert, M.K., Rubey, W.W., 1959. Role of Fluid Pressure in Mechanics of Overthrust Faulting I. Mechanics of Fluid-Filled Porous Solids and Its Application to Overthrust Faulting. Geol. Soc. Am. Bull. 70, 115–166. doi:10.1130/0016-7606(1959)70[115:ROFPIM]2.0.CO;2

Keranen, K.M., Savage, H.M., Abers, G.A., Cochran, E.S., 2013. Potentially induced earthquakes in Oklahoma, USA: Links between wastewater injection and the 2011 Mw 5.7 earthquake sequence. Geology 41, 699–702. doi:10.1130/G34045.1

Keranen, K.M., Weingarten, M., Abers, G.A., Bekins, B.A., Ge, S., 2014. Sharp increase in central Oklahoma seismicity since 2008 induced by massive wastewater injection. Science 345, 448–451. doi:10.1126/science.1255802

Kim, W.-Y., 2013. Induced seismicity associated with fluid injection into a deep well in Youngstown, Ohio. J. Geophys. Res. Solid Earth 118, 3506–3518. doi:10.1002/jgrb.50247

Klein, F.W., 2002. User's guide to HYPOINVERSE-2000, a Fortran program to solve for earthquake locations and magnitudes, USGS Open-File Report. 2002–171.

Laske, G., Masters, G., Ma, Z., Pasyanos, M., 2013. Update on CRUST1. 0—A 1-degree global model of Earth's crust, Geophys. Res. Abstracts. p. 20132658abstrEGU.

McNamara, D., Rubinstein, J., Myers, E., Smoczyk, G., Benz, H., Williams, R., Hayes, G., Wilson, D., Herrmann, R., McMahon, N., Aster, R., Bergman, E., Holland, A., Earle, P., 2015. Efforts to monitor and characterize the recent increasing seismicity in central Oklahoma. Lead. Edge 34, 628–639. doi:10.1190/tle34060628.1

Nayak, A., Dreger, D.S., 2014. Moment Tensor Inversion of Seismic Events Associated with the Sinkhole at Napoleonville Salt Dome, Louisiana. Bull. Seismol. Soc. Am. 104, 1763–1776. doi:10.1785/0120130260

Nicholson, C., Wesson, R.L., 1990. Earthquake hazard associated with deep well injection: a report to the U.S. Environmental Protection Agency, Bulletin. Washington, D.C. Report No. 1951.

Petersen, M.D., Frankel, A.D., Harmsen, S.C., Mueller, C.S., Haller, K.M., Wheeler, R.L., Wesson, R.L., Zeng, Y., Boyd, O.S., Perkins, D.M., Luco, N., Field, E.H., Wills, C.J., Rukstales, K.S., 2008. Documentation for the 2008 Update of the United States National Seismic Hazard Maps, USGS Open-File Report. 2008–1128.

Petersen, M.D., Moschetti, M.P., Powers, P.M., Mueller, C.S., Haller, K.M., Frankel, A.D., Zeng, Y., Rezaeian, S., Harmsen, S.C., Boyd, O.S., Field, N., Chen, R., Rukstales, K.S., Luco, N., Wheeler, R.L., Williams, R.A., Olsen, A.H., 2015. The 2014 United States National Seismic Hazard Model. Earthq. Spectra 31, S1–S30. doi:10.1193/120814EQS210M

Powell, C.A., Bollinger, G.A., Chapman, M.C., Sibol, M.S., Johnston, A.C., Wheeler, R.L., 1994. A seismotectonic model for the 300-kilometer-long eastern Tennessee seismic zone. Science 264, 686–689.

Powell, C.A., Thomas, W.A., 2016. Grenville basement structure associated with the Eastern Tennessee seismic zone, southeastern USA. Geology 44, 39–42. doi:10.1130/G37269.1

Raymond, D.E., Ebersole, S. M., Irvin, G. D., 2009. Basement fault maps of Alabama. Geological Society of America Abstracts with Programs 41, 12.

Raymond, D.E., Osborne, W.E., Copeland, C.W., Neathery, T.L., 1988. Alabama Stratigraphy, Circular 140. Geological Survey of Alabama, Stratigraphy and Paleontology Division.

Rubinstein, J.L., Mahani, A.B., 2015. Myths and Facts on Wastewater Injection, Hydraulic Fracturing, Enhanced Oil Recovery, and Induced Seismicity. Seismol. Res. Lett. 86, 1060–1067. doi:10.1785/0220150067

Seeber, L., Armbruster, J.G., Kim, W.-Y., Barstow, N., Scharnberger, C., 1998. The 1994 Cacoosing Valley earthquakes near Reading, Pennsylvania: A shallow rupture triggered by quarry unloading. J. Geophys. Res. Solid Earth 103, 24505–24521. doi:10.1029/98JB01497

Steigert, F.W., 1982. Seismicity of the southern Appalachian seismic zone in Alabama (Thesis). Georgia Institute of Technology.

Steltenpohl, M.G., Zietz, I., Horton, J.W., Daniels, D.L., 2010. New York–Alabama lineament: A buried right-slip fault bordering the Appalachians and mid-continent North America. Geology 38, 571–574. doi:10.1130/G30978.1

Sun, X., Yang, P., Zhang, Z., 2017. A study of earthquakes induced by water injection in the Changning salt mine area, SW China. J. Asian Earth Sci. 136, 102–109. doi:10.1016/j.jseaes.2017.01.030

Surles, D., 2007. Interactions between structures in the Appalachian and Ouachita foreland beneath the Gulf Coastal Plain (Dissertation). University of Kentucky.

Thomas, W.A., 2006. Tectonic inheritance at a continental margin. GSA Today 16, 4–11.

Tuttle, M.P., Schweig, E.S., Sims, J.D., Lafferty, R.H., Wolf, L.W., Haynes, M.L., 2002. The Earthquake Potential of the New Madrid Seismic Zone. Bull. Seismol. Soc. Am. 92, 2080–2089. doi:10.1785/0120010227

Waldhauser, F., 2001. HypoDD-A Program to Compute Double-Difference Hypocenter Locations, USGS Open-File Report. 2001–113.

Waldhauser, F., Ellsworth, W.L., 2000. A Double-Difference Earthquake Location Algorithm: Method and Application to the Northern Hayward Fault, California. Bull. Seismol. Soc. Am. 90, 1353–1368. doi:10.1785/0120000006

Walsh, F.R., Zoback, M.D., 2015. Oklahoma's recent earthquakes and saltwater disposal. Sci. Adv. 1, e1500195. doi:10.1126/sciadv.1500195

Weingarten, M., Ge, S., Godt, J.W., Bekins, B.A., Rubinstein, J.L., 2015. High-rate injection is associated with the increase in U.S. mid-continent seismicity. Science 348, 1336–1340. doi:10.1126/science.aab1345

Wilson, J.T., 1966. Did the Atlantic close and then re-open? Nature 211, 676-681.

Zhu, L., Helmberger, D.V., 1996. Advancement in source estimation techniques using broadband regional seismograms. Bull. Seismol. Soc. Am. 86, 1634–1641.

Zoback, M.D., Gorelick, S.M., 2012. Earthquake triggering and large-scale geologic storage of carbon dioxide. Proc. Natl. Acad. Sci. 109, 10164–10168. doi:10.1073/pnas.1202473109